which have costimulatory functions for the survival, expansion, and effector function of T cells, enhance systemic immunity to co-administered antigens [12]. However, there have been no comparative studies of the potential of TNF superfamily cytokines as mucosal vaccine adjuvants. To compare the mucosal adjuvant activities of TNF superfamily cytokines, we intranasally immunized mice with 100 μg OVA plus each of 16 different TNF superfamily cytokines (APRIL, BAFF, 4-1BBL, CD27L, CD30L, CD40L, EDA, GITRL, LIGHT, LT-α, OX40L, TL1A, TNF-α, TRAIL, TRANCE, and TWEAK; 1 μg/mouse) three times at weekly intervals. Intranasal immunization with OVA plus TL1A gave significantly higher OVA-specific IgG responses in the serum than did immunization with OVA alone (Fig. 31.3a). The OVA-specific IgG level in TL1A immunized mice was of similar magnitude to that induced by cholera toxin B subunit (CTB). In addition, intranasal immunization with OVA plus APRIL or TNF-α gave a strong OVA-specific IgG response in the serum. The highest OVA-specific IgG Ab responses were seen in mice immunized with OVA plus TL1A as a mucosal adjuvant, from

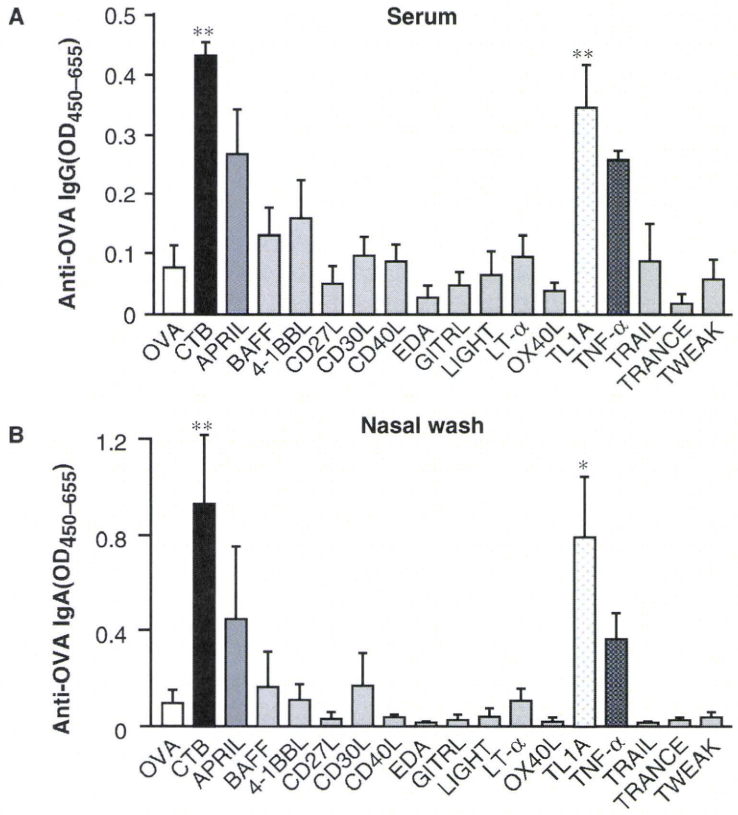

Fig. 31.3 OVA-specific Ig responses to intranasal immunization with ovalbumin (OVA) plus tumor necrosis factor (TNF) superfamily cytokines. BALB/c mice were intranasally immunized three times at weekly intervals with OVA alone, OVA plus cholera toxin B subunit (CTB), or OVA plus each TNF superfamily cytokine. Serum and nasal wash were collected 7 days after the last immunization and analyzed by ELISA for OVA-specific (**a**) IgG at a 500-fold dilution and OVA-specific (**b**) IgA at a 50-fold dilution. Data are presented as means ± SEM ($n = 5$; * $P < 0.05$, ** $P < 0.01$ versus value for group treated with OVA alone, by ANOVA)

among 16 different TNF superfamily cytokines (Fig. 31.3a). Next, to identify the characteristics of TNF superfamily cytokines as mucosal adjuvants, we examined OVA-specific IgA responses in nasal washes. Mice immunized with OVA plus APRIL or TNF-α tended to show strong OVA-specific IgA responses. Importantly, the OVA-specific IgA level was significantly higher in TL1A-immunized mice than in mice immunized with OVA alone; the level was similar to that induced by CTB (Fig. 31.3b). Collectively, these results demonstrated that TL1A was the most potent mucosal adjuvant among the TNF superfamily cytokines for inducing OVA-specific systemic IgG and mucosal IgA Ab responses; TL1A might therefore be candidate for a mucosal vaccine adjuvant to replace toxin-based adjuvants.

Next, to clarify the mechanisms of the immune response to the addition of each TNF superfamily cytokine, we analyzed the release profiles of cytokines from splenocytes of immunized mice. Culture supernatants from OVA-stimulated splenocytes collected from immunized mice were assessed for the Th2-type cytokines IL-4 and IL-5 and the Th1-type cytokines IFN-γ and TNF-α, using a multiplexed immunobead-based assay. Splenocytes from mice immunized with OVA plus APRIL, TNF-α, or TL1A exhibited higher levels of Th2-type cytokines (IL-4 and IL-5) than those immunized with OVA alone. In contrast, there was little difference in Th1-type cytokine (IFN-γ and TNF-α) secretion among all types of immunized mice. These results suggested that the addition of APRIL, TNF-α, or TL1A as a mucosal vaccine adjuvant induced a strongly polarized Th2-type immune response. Collectively, our results indicated that TL1A induced the strongest mucosal immunity among the TNF superfamily cytokines. This is the first report to demonstrate the activity of TL1A as a mucosal adjuvant inducing antigen-specific systemic and mucosal immune responses in mice.

Concluding Remarks

To our knowledge, this study is the first to clearly demonstrate the potential of TNF superfamily cytokines as mucosal adjuvants. In summary, among the TNF superfamily cytokines, APRIL, TL1A, and TNF-α induced two layers of protective immunity when administered intranasally with a vaccine antigen. TL1A was more effective than other TNF superfamily cytokines as a mucosal vaccine adjuvant. In the future, application of our technology to the creation of mutant TL1A could lead to the generation of a promising mucosal adjuvant that is both effective and safe.

Acknowledgments This study was supported in part by Grants-in-Aid for Scientific Research from the Ministry of Education, Culture, Sports, Science, and Technology of Japan, and from the Japan Society for the Promotion of Science (JSPS). The study was also supported in part by Health Labor Sciences Research Grants from the Ministry of Health, Labor, and Welfare of Japan; by Health Sciences Research Grants for Research on Publicly Essential Drugs and Medical Devices, from the Japan Health Sciences Foundation.

References

1. Ada G (2001) Vaccines and vaccination. N Engl J Med 345:1042–1053
2. Brandtzaeg P (2007) Induction of secretory immunity and memory at mucosal surfaces. Vaccine 25:5467–5484
3. Eriksson K, Holmgren J (2002) Recent advances in mucosal vaccines and adjuvants. Curr Opin Immunol 14:666–672
4. Gorbach SL, Khurana CM (1971) Toxigenic *Escherichia coli* in infantile diarrhea in Chicago. J Lab Clin Med 78:981–982
5. Hehlgans T, Pfeffer K (2005) The intriguing biology of the tumour necrosis factor/tumour necrosis factor receptor superfamily: players, rules and the games. Immunology 115:1–20
6. Holmgren J, Czerkinsky C (2005) Mucosal immunity and vaccines. Nat Med 11:S45–S53
7. Kayamuro H, Abe Y, Yoshioka Y et al (2009a) The use of a mutant TNF-alpha as a vaccine adjuvant for the induction of mucosal immune responses. Biomaterials 30:5869–5876
8. Kayamuro H, Yoshioka Y, Abe Y et al (2009b) TNF superfamily member, TL1A, is a potential mucosal vaccine adjuvant. Biochem Biophys Res Commun 384:296–300
9. Mutsch M, Zhou W, Rhodes P et al (2004) Use of the inactivated intranasal influenza vaccine and the risk of Bell's palsy in Switzerland. N Engl J Med 350:896–903
10. Neutra MR, Kozlowski PA (2006) Mucosal vaccines: the promise and the challenge. Nat Rev Immunol 6:148–158
11. Shibata H, Yoshioka Y, Ikemizu S et al (2004) Functionalization of tumor necrosis factor-alpha using phage display technique and PEGylation improves its antitumor therapeutic window. Clin Cancer Res 10:8293–8300
12. Tamada K, Chen L (2006) Renewed interest in cancer immunotherapy with the tumor necrosis factor superfamily molecules. Cancer Immunol. Immunother 55:355–362

JOURNAL OF VIROLOGY, Dec. 2010, p. 12703–12712 Vol. 84, No. 24
0022-538X/10/$12.00 doi:10.1128/JVI.01182-10

Interleukin-1 Family Cytokines as Mucosal Vaccine Adjuvants for Induction of Protective Immunity against Influenza Virus[▽]

Hiroyuki Kayamuro,[1,2]† Yasuo Yoshioka,[1,3]† Yasuhiro Abe,[1]† Shuhei Arita,[1,2] Kazufumi Katayama,[4] Tetsuya Nomura,[1] Tomoaki Yoshikawa,[1,2] Ritsuko Kubota-Koketsu,[5] Kazuyoshi Ikuta,[5] Shigefumi Okamoto,[6] Yasuko Mori,[6] Jun Kunisawa,[7] Hiroshi Kiyono,[7] Norio Itoh,[2] Kazuya Nagano,[1] Haruhiko Kamada,[1,3] Yasuo Tsutsumi,[1,2,3] and Shin-Ichi Tsunoda[1,3]*

Laboratory of Biopharmaceutical Research, National Institute of Biomedical Innovation, 7-6-8 Saito-Asagi, Ibaraki, Osaka 567-0085, Japan[1]; Department of Toxicology and Safety Science, Graduate School of Pharmaceutical Sciences, Osaka University, 1-6 Yamadaoka, Suita, Osaka 565-0871, Japan[2]; The Center for Advanced Medical Engineering and Informatics, Osaka University, 1-6 Yamadaoka, Suita, Osaka 565-0871, Japan[3]; Department of Biochemistry and Molecular Biology, Graduate School of Pharmaceutical Sciences, Osaka University, 1-6 Yamadaoka, Suita, Osaka 565-0871, Japan[4]; Department of Virology, Research Institute for Microbial Diseases, Osaka University, 3-1 Yamadaoka, Suita, Osaka 565-0871, Japan[5]; Laboratory of Virology and Vaccinology, Division of Biomedical Research, National Institute of Biomedical Innovation, 7-6-8 Saito-Asagi, Ibaraki, Osaka 567-0085, Japan[6]; and Division of Mucosal Immunology, Department of Microbiology and Immunology, The Institute of Medical Science, The University of Tokyo, 4-6-1 Shirokanedai, Minato-ku, Tokyo 108-8639, Japan[7]

Received 2 June 2010/Accepted 22 September 2010

A safe and potent adjuvant is needed for development of mucosal vaccines against etiological agents, such as influenza virus, that enter the host at mucosal surfaces. Cytokines are potential adjuvants for mucosal vaccines because they can enhance primary and memory immune responses enough to protect against some infectious agents. For this study, we tested 26 interleukin (IL) cytokines as mucosal vaccine adjuvants and compared their abilities to induce antigen (Ag)-specific immune responses against influenza virus. In mice intranasally immunized with recombinant influenza virus hemagglutinin (rHA) plus one of the IL cytokines, IL-1 family cytokines (i.e., IL-1α, IL-1β, IL-18, and IL-33) were found to increase Ag-specific immunoglobulin G (IgG) in plasma and IgA in mucosal secretions compared to those after immunization with rHA alone. In addition, high levels of both Th1- and Th2-type cytokines were observed in mice immunized with rHA plus an IL-1 family cytokine. Furthermore, mice intranasally immunized with rHA plus an IL-1 family cytokine had significant protection against a lethal influenza virus infection. Interestingly, the adjuvant effects of IL-18 and IL-33 were significantly decreased in mast cell-deficient *W/W*^{v} mice, indicating that mast cells have an important role in induction of Ag-specific mucosal immune responses induced by IL-1 family cytokines. In summary, our results demonstrate that IL-1 family cytokines are potential mucosal vaccine adjuvants and can induce Ag-specific immune responses for protection against pathogens like influenza virus.

Because most pathogenic viruses, including influenza virus, enter through a mucosal surface (18), preventing infection at the viral entry site by inducing mucosal immunity should be an effective strategy for combating such pathogens. A key aspect of mucosal immunity is production of secretory immunoglobulin A (sIgA), as well as induction of cytolytic T lymphocytes (CTLs) against epithelium-transmitted pathogens (5, 21). Therefore, it is important to develop mucosal vaccines that induce effective immune responses at mucosal surfaces (31).

However, protein subunit antigens (Ags) generally evoke only a weak or undetectable adaptive immune response when administered intramucosally (1). Therefore, to produce effective mucosal vaccines, it is necessary to develop an appropriate mucosal vaccine adjuvant (34). Cholera toxin (CT) and *Escherichia coli* heat-labile enterotoxin are known potent mucosal vaccine adjuvants and have been used in nonclinical experimental systems (9, 27). However, their clinical application as nasal adjuvants had to be discontinued because of side effects such as Bell's palsy (29). Therefore, mucosal vaccine adjuvants with high efficacy and safety for clinical application continue to be urgently required.

Cytokines are key molecules that trigger the innate and adaptive immune responses (including maturation of Ag-presenting cells, differentiation of Th1 and Th2 cells, and induction of cytotoxic natural killer [NK] cells and CTLs), resulting in protective layers against virus infection (11, 41, 43). Therefore, cytokines are promising vaccine adjuvants for enhancing the immune response against infectious pathogens. At present, more than 30 members of the interleukin (IL) cytokine/IL receptor family have been identified and found to be involved

* Corresponding author. Mailing address: Laboratory of Biopharmaceutical Research, National Institute of Biomedical Innovation, 7-6-8 Saito-Asagi, Ibaraki, Osaka 567-0085, Japan. Phone: 81-72-641-9811. Fax: 81-72-641-9817. E-mail: tsunoda@nibio.go.jp.
† H.K., Y.Y., and Y.A. contributed equally to this work.
▽ Published ahead of print on 29 September 2010.

in regulating and maintaining homeostasis of the immune system (3, 14). Specific IL cytokines have been used as vaccine adjuvants to enhance primary and memory immune responses against some cancers and infectious diseases (2, 6). However, there has been no comparative study of IL cytokines as mucosal vaccine adjuvants.

Recently, it was pointed out that identification of the cellular targets of vaccine adjuvants is an important issue (12). Dendritic cells (DCs) are responsible for Ag uptake and presentation to naive T cells and represent a key target for adjuvant activity (22, 33). Recent reports have demonstrated that other accessory cells, such as mast cells (MCs) and NKT cells, act as immunosensors to initiate and modulate innate and adaptive immune responses (16, 40). It has been reported that MCs contribute to the induction of an adaptive immune response or accessory function and that the synthetic Toll-like receptor 7 ligand imiquimod acts as a mucosal vaccine adjuvant in an MC-dependent manner (19). However, it is still not clear whether MCs are promising cellular targets for cytokine adjuvants in mucosal vaccines.

In this study to develop effective and safe mucosal vaccine adjuvants, we identified promising cytokines with mucosal vaccine adjuvant activity by screening 26 different IL cytokines. We also investigated the mucosal and systemic immune responses induced by these cytokines in normal and MC-deficient mice. The IL-1 family cytokines (IL-1α, IL-1β, IL-18, and IL-33) were found to be effective mucosal vaccine adjuvants for induction of protective sIgA and CTL immunity against influenza virus. In addition, the adjuvant activities of IL-18 and IL-33 were MC dependent.

MATERIALS AND METHODS

Cytokines and Ags. CT was purchased from List Biological Laboratories (Campbell, CA). Twenty-six types of mouse recombinant IL cytokines (IL-1α, IL-1β, IL-2, IL-3, IL-4, IL-5, IL-6, IL-7, IL-9, IL-10, IL-11, IL-12, IL-13, IL-15, IL-17, IL-18, IL-19, IL-20, IL-21, IL-22, IL-23, IL-27, IL-28A, IL-28B, IL-31, and IL-33) were purchased from R&D Systems (Minneapolis, MN). Baculovirus-expressed recombinant influenza virus hemagglutinin (rHA) derived from influenza virus A/New Caledonia/20/1999 (Protein Sciences, Meriden, CT) was used as the vaccine Ag.

Mice and immunization protocols. Female BALB/c mice and MC-deficient (WBB6F1 *W/W*^{v}) and congenic littermate control (WBB6F1 WT) mice were purchased from Japan SLC (Hamamatsu, Japan) and used at 6 weeks of age. All animal experimental procedures used in this study were performed in accordance with our institutional guidelines for animal experiments. Mice were immunized intranasally with rHA alone (1 μg/mouse), rHA (1 μg/mouse) plus CT (1 μg/mouse), or rHA (1 μg/mouse) plus one of the IL cytokines (0.1 μg, 0.3 μg, or 1.0 μg/mouse) on days 0 and 28.

Sample collection. Fourteen days after the final immunization, plasma and mucosal secretions (nasal washes, saliva, vaginal washes, and fecal extracts) were obtained as previously described (24).

Detection of Ab responses by ELISA. rHA-specific antibody (Ab) levels in plasma and mucosal secretions were determined by enzyme-linked immunosorbent assay (ELISA) as previously described (24). Briefly, ELISA plates were coated with 2 μg rHA/ml of 0.1 M carbonate buffer and incubated overnight at 4°C. The plates were then incubated with blocking solution (Block Ace; DS Pharma Biomedical, Osaka, Japan) at 37°C for 2 h. Diluted plasma or mucosal secretions were added. After incubation at 37°C for 2 h, the coated plates were washed with phosphate-buffered saline (PBS)–polyoxyethylene sorbitan monolaurate (Tween 20; Wako Pure Chemical, Tokyo, Japan) and incubated with horseradish peroxidase (HRP)-conjugated goat anti-mouse IgG solution to detect IgG in plasma or with a biotin-conjugated goat anti-mouse IgA detection Ab (Southern Biotechnology Associates, Birmingham, AL) solution to detect sIgA in mucosal secretions, at 37°C for 2 h. For detection of sIgA, the plates were incubated with HRP-coupled streptavidin (Zymed Laboratories, South San Francisco, CA) for 1 h at room temperature. After incubation, a color reaction was developed with tetramethylbenzidine (Moss, Inc., Pasadena, MD), stopped with 2 N H_2SO_4, and measured as the optical density at 450 to 655 nm ($OD_{450-655}$) in a microplate reader.

Multiplex cytokine assay. Splenocytes from immunized BALB/c, WBB6F1 *W/W*^{v}, or WBB6F1 WT mice were harvested 14 days after the final immunization and stimulated *in vitro* with 10 μg rHA/ml. After 72 h, culture supernatants from *in vitro* unstimulated and rHA-stimulated cells were analyzed by a Bio-Plex multiplex cytokine assay (Bio-Rad Laboratories, Hercules, CA) according to the manufacturer's instructions. Samples were analyzed on a Luminex 100 analyzer (Luminex, Austin, TX). The mean concentrations of cytokines in supernatants from rHA-stimulated cells were calculated relative to those in unstimulated cells.

IFN-γ ELISPOT assay. Splenocytes from immunized mice were harvested 14 days after the final immunization and stimulated at a cell density of 1×10^7 cells/ml with a mixture of two H-2K^{d}-restricted class I HA peptides, $HA_{240-248}$ (IYSTVASSL) and $HA_{462-470}$ (LYEKVKSQL) (MBL, Nagoya, Japan), at a final concentration of 10 μg total peptide/ml complete RPMI (25). After 24 h of incubation at 37°C, plates were washed, and gamma interferon (IFN-γ)-producing cells were measured by use of an enzyme-linked immunospot (ELISPOT) assay kit (BD Biosciences, San Diego, CA) according to the manufacturer's instructions.

Tetramer assay. Splenocytes from immunized mice were harvested 14 days after the final immunization and used as effector cells to determine $HA_{240-248}$-specific CTL responses. Splenocytes (7×10^6 cells) were added to wells in a 24-well plate, followed by addition of 1 ml of medium containing a CTL epitope peptide ($HA_{240-248}$; IYSTVASSL) at a final concentration of 1 μg/ml. After incubation at 37°C for 2 days, medium containing human recombinant IL-2 (rIL-2) (Shionogi Co., Osaka, Japan) was added to each well of CTL effector cells, to a final concentration of 10 U human rIL-2/ml. Effector cells were stained for tetramers after restimulation for 7 days. For analysis, 1×10^6 cells were treated with purified anti-mouse CD16/CD32 Ab (Fc-γ III/II receptor Ab; BD Biosciences Pharmingen, San Diego, CA) and then stained with phycoerythrin (PE)-conjugated H-2K^{d}-$HA_{240-248}$ peptide tetramer (MBL, Nagoya, Japan) for 20 min at room temperature. Fluorescein isothiocyanate (FITC)-conjugated CD8α (clone KT15; MBL, Nagoya, Japan) was added for an additional 20 min. Cells were analyzed with a FACS Canto flow cytometer (BD Biosciences Pharmingen). Data analysis was done with FlowJo (TreeStar, Eugene, OR) software.

Histopathological analysis. BALB/c mice were immunized intranasally with rHA (1 μg/mouse), with or without IL-1α, IL-1β, IL-18, or IL-33 (1 μg/mouse), on days 0 and 28. Fourteen days after the final immunization, the heads of the mice were severed from the bodies and placed in fixative solution (4% paraformaldehyde). The samples then were sectioned and stained with hematoxylin and eosin (H&E) or Luna stain and examined for pathological changes under a light microscope. Histopathological examination was performed by the Applied Medical Research Laboratory (Osaka, Japan).

Influenza virus infection *in vivo*. To examine the prophylactic effect of IL cytokine treatment against influenza virus, mice were immunized intranasally on days 0 and 28 with 1 μg PR8 HA vaccine (inactivated-product vaccine with influenza virus A/Puerto Rico/8/34) (Charles River, North Franklin, CT)/mouse plus 1 μg CT or IL-1 family cytokine/mouse. Fourteen days after the final immunization, mice were fully anesthetized by intraperitoneal injection of pentobarbital, and each was infected by intranasal application of 25 μl PBS containing 256 hemagglutinating units (HAU) of influenza virus A/PR/8/34 (H1N1) (kindly provided by the Research Institute for Microbial Diseases of Osaka University, Osaka, Japan) per mouse. This procedure produced upper and lower respiratory tract infections.

Statistical analysis. All results are expressed as means ± standard errors of the means (SEM). Differences were compared using Bonferroni analysis of variance (ANOVA).

RESULTS

Comparative analysis of rHA-specific Ab responses induced by 26 different IL cytokines. One potential advantage of successful mucosal immunization is the possibility of eliciting both systemic IgG and mucosal sIgA Ab responses against invading pathogens. Therefore, in this study, we tested 26 different IL cytokines (IL-1α, IL-1β, IL-2, IL-3, IL-4, IL-5, IL-6, IL-7, IL-9, IL-10, IL-11, IL-12, IL-13, IL-15, IL-17, IL-18, IL-19, IL-20, IL-21, IL-22, IL-23, IL-27, IL-28A, IL-28B, IL-31, and IL-33)

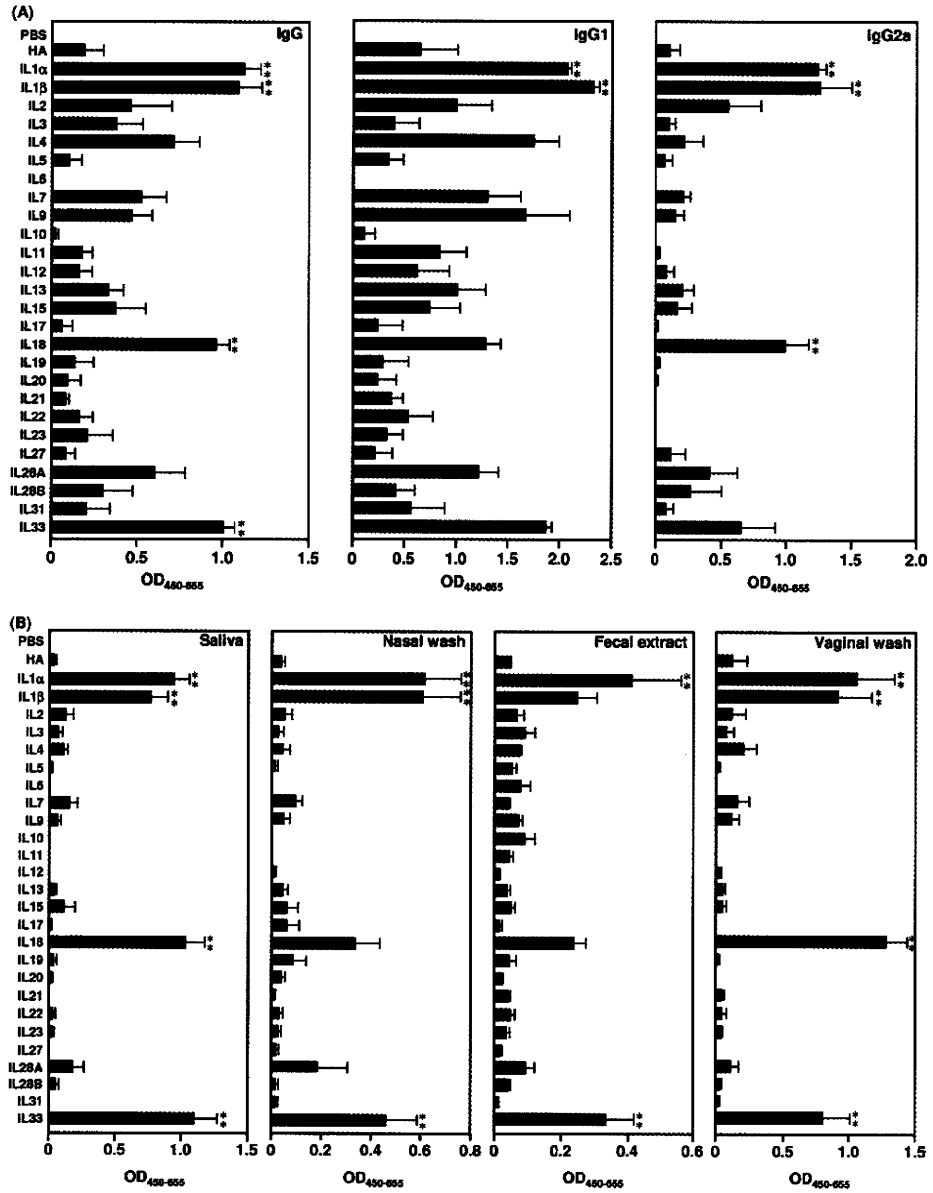

FIG. 1. Ab responses induced by IL-1 family cytokines. BALB/c mice were immunized intranasally at 0 and 28 days with rHA alone or rHA plus each interleukin. (A) Plasma was collected 14 days after the final immunization and analyzed by ELISA for rHA-specific IgG, IgG1, and IgG2a. (B) Saliva, nasal washes, fecal extracts, and vaginal washes were collected 14 days after the final immunization and analyzed by ELISA for rHA-specific sIgA. Data are presented as means ± SEM ($n = 5$). **, $P < 0.01$ compared to the value for the rHA-treated group.

as mucosal vaccine adjuvants. To examine the potential of these IL cytokines as mucosal vaccine adjuvants, BALB/c mice were immunized intranasally with 1 μg rHA plus 1 μg of an IL cytokine on days 0 and 28. Fourteen days after the final immunization, we examined the level of anti-rHA IgG in plasma by ELISA (Fig. 1A). Intranasal immunization with rHA plus 11 of the IL cytokines (IL-1α, IL-1β, IL-2, IL-3, IL-4, IL-7, IL-9, IL-13, IL-15, IL-18, IL-28A, and IL-33) induced higher rHA-specific IgG responses in plasma than those for mice immunized with rHA alone (Fig. 1A). In particular, immunization with rHA plus IL-1α, IL-1β, IL-18, or IL-33, referred to as IL-1 family cytokines, resulted in the highest rHA-specific IgG responses among the IL cytokines. The IgG subclass of the rHA-specific responses was then examined to assess the type of immune response induced by the 26 IL cytokines (Fig. 1A). Plasma Ag-specific IgG subclasses reflect the subset of $CD4^+$ T-helper cells induced by vaccination, with IgG1 and IgG2a corresponding to Th2 and Th1 responses, respectively. Consistent with the rHA-specific IgG responses, intranasal immunization with rHA plus IL-2, IL-3, IL-4, IL-7, IL-9, IL-13, IL-15, or IL-28A generally produced a greater rHA-specific IgG1 subclass response than immunization with rHA alone but a similar IgG2a response to that with rHA alone. In contrast, mice immunized with rHA plus IL-1 family cytokines showed

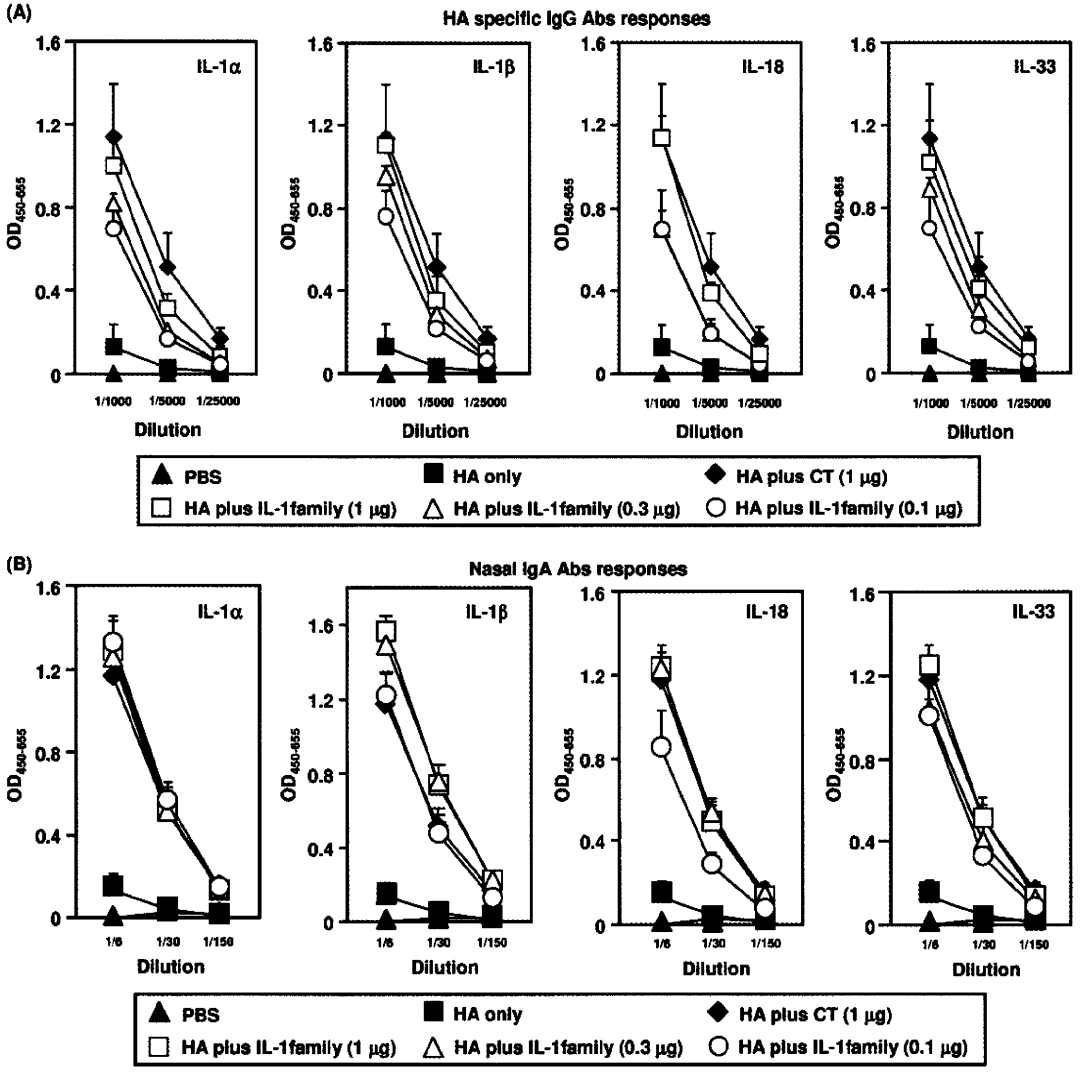

FIG. 2. Dose-response relationship for induction of rHA-specific Ab responses by nasal immunization with rHA plus an IL-1 family cytokine. BALB/c mice were immunized intranasally at 0 and 28 days with rHA alone, rHA plus CT (1 μg/mouse), or rHA plus an IL-1 family cytokine (0.1, 0.3, or 1 μg/mouse). (A) Plasma was collected 14 days after the final immunization and analyzed by ELISA for rHA-specific IgG, at dilutions of 1/1,000, 1/5,000, and 1/250,000. (B) Nasal washes were collected 14 days after the final immunization and analyzed by ELISA for rHA-specific sIgA, at dilutions of 1/6, 1/30, and 1/150. Data are presented as means ± SEM (n = 5).

significantly higher IgG1 and IgG2a Ab responses than those immunized with rHA alone. These results indicate that nasal administration of IL-1 family cytokines has the potential to induce potent rHA-specific systemic IgG Abs, as well as IgG1 and IgG2a Ab responses. We then studied the rHA-specific sIgA response in mucosal secretions (i.e., in saliva, nasal washes, fecal extracts, and vaginal washes) induced by the 26 IL cytokines (Fig. 1B). For these 26 IL cytokines, IL-1 family cytokines induced the highest mucosal sIgA Ab responses in salivary, nasal, fecal, and vaginal mucosal secretions (Fig. 1B). Taken together, these results indicate that nasal immunization with IL-1 family cytokines effectively induced rHA-specific Ab responses in both systemic and mucosal immune compartments, suggesting that IL-1 family cytokines might be effective mucosal vaccine adjuvants.

Dose-response relationship of IL-1 family cytokines as mucosal vaccine adjuvants for induction of rHA-specific Ab responses. To determine the dose-response relationship of IL-1 family cytokines as mucosal vaccine adjuvants to induce rHA-specific IgG and sIgA Ab responses, mice were immunized intranasally with rHA plus 0.1, 0.3, or 1 μg of each IL-1 family cytokine (Fig. 2). Immunization with rHA plus the IL-1 family cytokines induced rHA-specific IgG in plasma in a dose-dependent manner. Even rHA plus the lowest dose (0.1 μg) of IL-1 family cytokines induced IgG to levels significantly higher than those induced by rHA alone (Fig. 2A). Importantly, the use of 1 μg of IL-1 family cytokines as an adjuvant resulted in

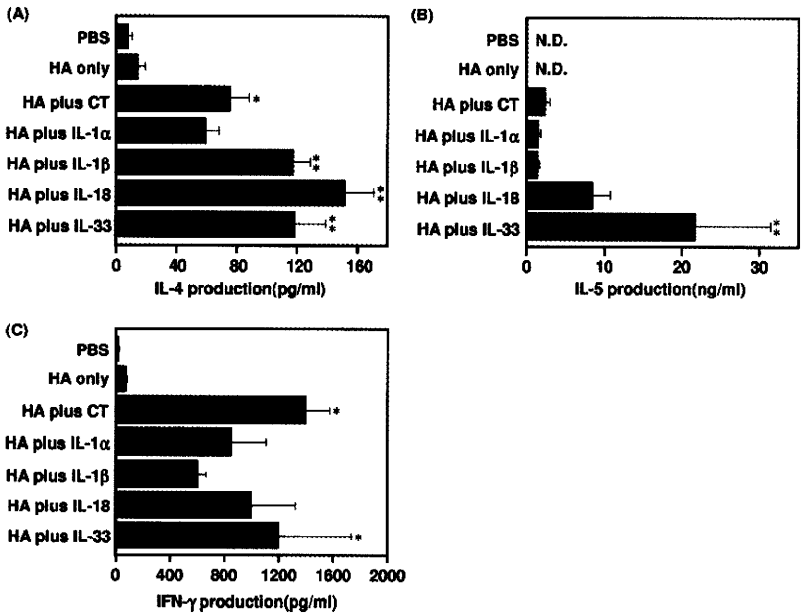

FIG. 3. Cytokine responses induced by nasal immunization with rHA plus IL-1 family cytokines. BALB/c mice were immunized intranasally at 0 and 28 days with rHA alone, rHA plus CT, or rHA plus an IL-1 family cytokine. Fourteen days after the final immunization, splenocytes from each group were cultured with 10 μg rHA/ml. Culture supernatants were harvested after a 3-day incubation and then assayed for rHA-specific IL-4 (A), IL-5 (B), and IFN-γ (C), using a Bio-Plex multiplex cytokine assay. Data are presented as means ± SEM ($n = 5$). *, $P < 0.05$; **, $P < 0.01$ compared to the value for the rHA-treated group. N.D., not done.

strong rHA-specific IgG Ab responses equivalent to those elicited by CT, which is one of the most potent mucosal vaccine adjuvants (Fig. 2A). Furthermore, the level of rHA-specific sIgA induced by rHA plus 0.1 μg of each IL-1 family cytokine in nasal secretions was significantly higher than that induced by rHA alone (Fig. 2B). The level of rHA-specific nasal sIgA induced in mice immunized intranasally with rHA plus 0.3 μg of each IL-1 family cytokine was equivalent to that observed in mice treated with 1 μg CT. Taken together, these results clearly indicate that nasal immunization with an IL-1 family cytokine as a mucosal vaccine adjuvant induced dose-dependent levels of both rHA-specific IgG and sIgA Abs in the mucosal and systemic immune compartments.

Induction of rHA-specific Th1- and Th2-type responses after nasal administration of IL-1 family cytokines as mucosal vaccine adjuvants. To evaluate the ability of IL-1 family cytokines to boost rHA-specific cytokine responses induced by mucosal immunization, splenocytes from mice that had been immunized intranasally with rHA alone, rHA plus CT, or rHA plus an IL-1 family cytokine were restimulated *in vitro* with rHA and then assayed for Th1 (IFN-γ) and Th2 (IL-4 and IL-5) cytokines (Fig. 3). Splenocytes from mice immunized with rHA alone did not show significant cytokine production compared to those from PBS-treated mice. Consistent with the IgG subclass results (Fig. 1A), mice immunized with IL-1 family cytokines had higher levels of IL-4 and IL-5 (Th2-associated sIgA-enhancing cytokines) than mice given rHA alone. In particular, the highest levels of IL-4 and IL-5 were detected in splenocytes of mice immunized with rHA plus IL-18 or IL-33, and these responses were significantly higher than those in splenocytes of mice immunized with CT. It was also noteworthy that IFN-γ, a Th1 cytokine, was induced in mice immunized intranasally with rHA plus an IL-1 family cytokine. Thus, IL-1 family cytokines might induce CTL responses when administered nasally. These results show that as mucosal vaccine adjuvants, IL-1α, IL-1β, IL-18, and IL-33 elicit both Th1- and Th2-type cytokine responses.

***In vivo* CTL induction by nasal immunization with rHA plus IL-1 family cytokines as mucosal vaccine adjuvants.** Virus clearance is known to require strong Th1-polarized immune responses characterized by IFN-γ production and CTL responses in the systemic compartment. To investigate the ability of IL-1 family cytokines to act as mucosal vaccine adjuvants and to induce rHA-specific Th1/CTL immune responses, we measured H-2K^d/HA$_{240-248}$ tetramer$^+$ CD8$^+$ T cells (Fig. 4A) and H-2K^d/HA$_{240-248}$-specific IFN-γ-secreting cells (Fig. 4B) in splenocytes from mice that had been immunized intranasally with rHA alone, rHA plus CT, or rHA plus an IL-1 family cytokine. The level of H-2K^d/HA$_{240-248}$ tetramer$^+$ CD8$^+$ T cells induced by rHA plus IL-1β was found to be similar to that induced by rHA alone, but the level induced by rHA plus IL-1α, IL-18, or IL-33 was significantly greater than that induced by rHA alone (Fig. 4A). Furthermore, the level of functionally active H-2K^d/HA$_{240-248}$-specific IFN-γ-secreting cells induced by rHA plus IL-1α, IL-18, or IL-33 was the same as or greater than that in mice intranasally immunized with rHA plus CT (Fig. 4B). Taken together, these results indicate that the IL-1 family cytokines IL-1α, IL-18 and IL-33 induce high-avidity CD8$^+$ CTLs. Therefore, intranasally administered IL-1α, IL-18, and IL-33 might be useful adjuvants for development of an effective mucosal influenza vaccine.

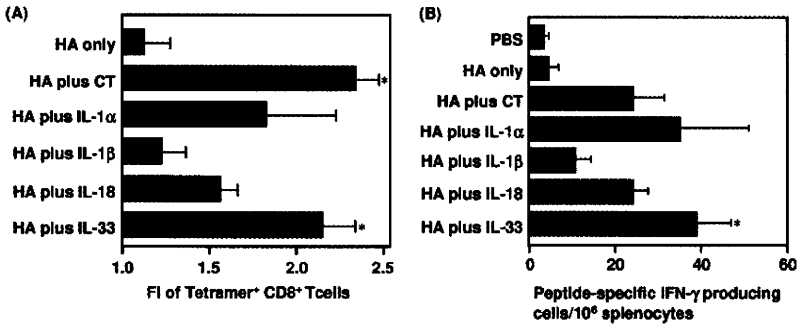

FIG. 4. Measurement of H-2K^d/HA$_{240-248}$ tetramer$^+$ CD8$^+$ T cells and H-2K^d/HA$_{240-248}$-specific IFN-γ-secreting cells in the spleen after nasal immunization with rHA plus an IL-1 family cytokine. BALB/c mice were immunized intranasally at 0 and 28 days with rHA alone, rHA plus CT, or rHA plus an IL-1 family cytokine. Fourteen days after the final immunization, splenocytes from immunized mice were harvested and stimulated with H-2K^d-restricted class I HA peptide at a final concentration of 10 μg total peptide/ml. (A) For detection of H-2K^d/HA$_{240-248}$ tetramer$^+$ CD8$^+$ T cells, splenocytes from immunized mice were cultured in medium containing a CTL epitope peptide (HA$_{240-248}$; IYSTVASSL) plus 10 U human IL-2/ml for 7 days, stained for CD8, and analyzed for tetramer-binding cells by flow cytometry. FI, fluorescence intensity. (B) After 24 h of incubation, IFN-γ-producing cells were measured by an ELISPOT assay. Data are presented as means ± SEM (n = 5). *, $P < 0.05$ compared to the value for the rHA-treated group.

Histopathological changes due to IL-1 family cytokines administered intranasally as mucosal vaccine adjuvants. Although enterotoxin-based adjuvants show strong mucosal immunity-inducing ability, they have significant toxic side effects on the central nervous system due to the presence of a specific receptor, GM1 ganglioside, which is highly expressed in neuronal tissue (39). To evaluate the *in vivo* toxicity of IL-1 family cytokines, histopathological changes in nasal tissues of mice given 1 μg of IL-1 family cytokines were investigated. No histological changes indicative of severe inflammation or membrane barrier disruption were observed in the nasal cavities of mice nasally administrated 1 μg of an IL-1 family cytokine (Fig. 5A). In particular, there was no evidence of massive accumulations of mononuclear cells around the airways and blood vessels or of infiltrates in the nasal tissues for all mice examined. Importantly, mice immunized intranasally with IL-1 family cytokines did not induce the goblet cell hyperplasia observed in patients with asthma and chronic obstructive pulmonary disease. Furthermore, Luna staining revealed that IL-1 family cytokine-treated mice did not develop infiltration of Luna-stained eosinophils into the nasal septum (Fig. 5B). Although further evaluation is required, these results indicate that the toxicity of IL-1 family cytokines is likely to be relatively low.

Antiviral immune response to influenza virus infection in mice after nasal immunization with IL-1 family cytokines as mucosal vaccine adjuvants. To determine the level of protection against viral infection provided by IL-1 family cytokines, BALB/c mice were immunized intranasally with 1 μg PR8 HA alone or with 1 μg of an IL-1 family cytokine on days 0 and 28. The immunized mice were then challenged with 256 HAU of mouse-adapted PR8 virus 14 days after the final immunization. The survival and weight of the infected mice were observed every other day (Fig. 6). All mice in the group receiving PBS alone and 86% of the mice immunized with PR8 HA alone died within 7 days of infection. In contrast, mice immunized intranasally with PR8 HA plus an IL-1 family cytokine showed a marked increase in survival (Fig. 6A). Notably, mice immunized with PR8 HA plus IL-1β or IL-18 had 100% survival 14 days after challenge, though with a slight loss of body weight (Fig. 6B). These results indicate that IL-1 family cytokines are potent nasal vaccine adjuvants for providing protection against viral infection.

Role of MCs in rHA-specific immune responses induced by nasal immunization with rHA plus IL-1 family cytokines. MCs are localized predominantly at the interface between the host and the environment (i.e., skin and mucosal surfaces). Recent reports have demonstrated the importance of IL-18-mediated MC activation for host defense, including innate sensing of pathogens (35) and recruitment of DCs and T lymphocytes to sites of inflammation. These findings prompted us to investigate whether MCs have a significant role in the immune response induced by IL-1 family cytokines as mucosal vaccine adjuvants. Hence, we examined MC-dependent rHA-specific systemic IgG and mucosal sIgA Ab responses induced by IL-1 family cytokine adjuvants. For this study, we compared the induction of specific Ab responses in MC-deficient (*W/W^v*) and WT mice immunized intranasally with rHA plus an IL-1 family cytokine (Fig. 7A and B). Both WT and *W/W^v* mice immunized with rHA had only minimal rHA-specific IgG Ab responses. However, rHA plus an IL-1 family cytokine induced significant rHA-specific IgG Ab responses in WT mice. *W/W^v* mice immunized with rHA plus IL-1α, IL-1β, or IL-33 also had significant rHA-specific IgG Ab responses (Fig. 7A), suggesting that IL-1α, IL-1β, and IL-33 act in an MC-independent manner. In contrast, the rHA-specific IgG Ab response induced in *W/W^v* mice by IL-18 was considerably lower than that in WT mice (Fig. 7A). Similar results were found for mucosal sIgA Ab responses: a significant response was seen with rHA plus IL-1α, IL-1β, or IL-33 in both WT and *W/W^v* mice, and a decreased response was seen with rHA plus IL-18 in *W/W^v* mice compared to WT mice (Fig. 7B). We then compared IL-4, IL-5, IL-2, and IFN-γ production in WT and *W/W^v* mice immunized with rHA plus IL-1 family cytokines (Fig. 7C). WT mice immunized with rHA plus IL-1 family cytokines showed significantly more rHA-specific IL-4, IL-5, IL-2, and IFN-γ production than did WT mice immunized with rHA alone. In contrast, the responses induced by rHA plus IL-18 were sig-

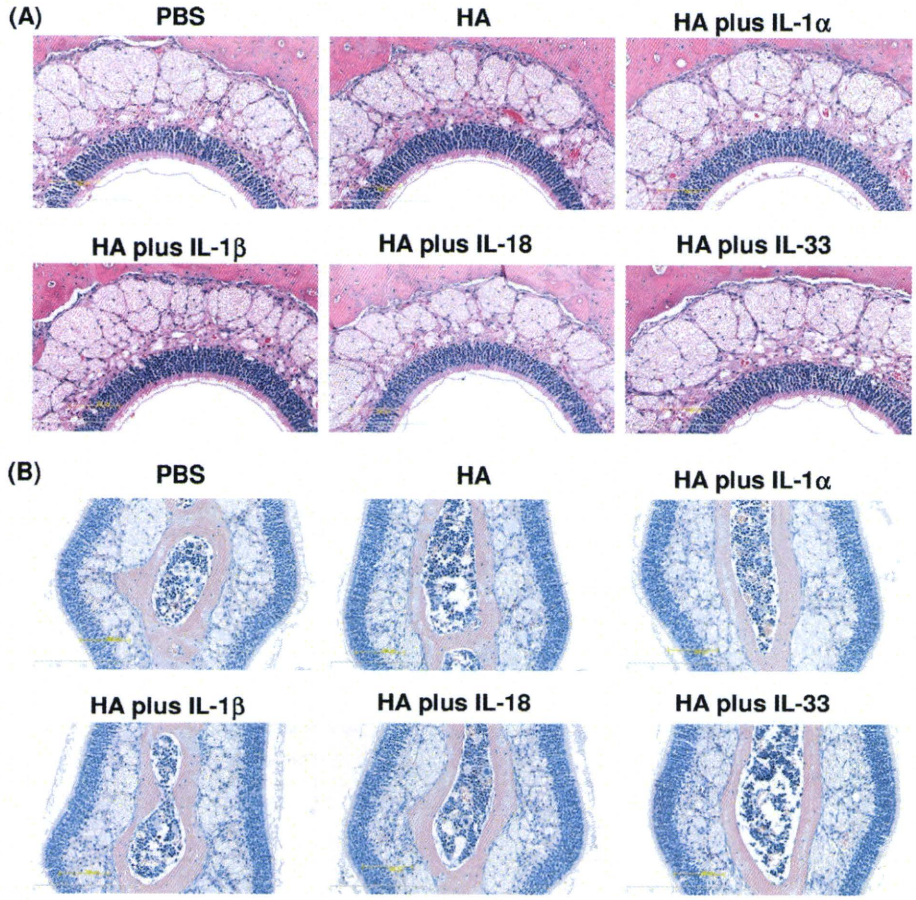

FIG. 5. Histopathological analysis of the nasal cavities of mice immunized intranasally with IL-1 family cytokines. Frontal cross sections of the nasal cavities of mice were taken after two administrations of PBS, rHA alone, or rHA plus an IL-1 family cytokine. Sections were prepared and stained with H&E (A) or Luna stain (B) to assess pathological changes. Overall views of the nasal epithelium (A) and of Luna-stained eosinophils in the nasal septum (B) are shown.

nificantly reduced in *W/W*^{v} mice. In addition, although rHA-specific IL-2, IL-4, and IL-5 production in *W/W*^{v} mice immunized with rHA plus IL-33 was comparable to that in WT mice, the rHA-specific IFN-γ response was significantly reduced in *W/W*^{v} mice. Collectively, these results indicate that MCs have a crucial role in the rHA-specific immune response induced by nasal immunization with rHA plus IL-18. In particular, MCs appear to have an important role in regulating rHA-specific

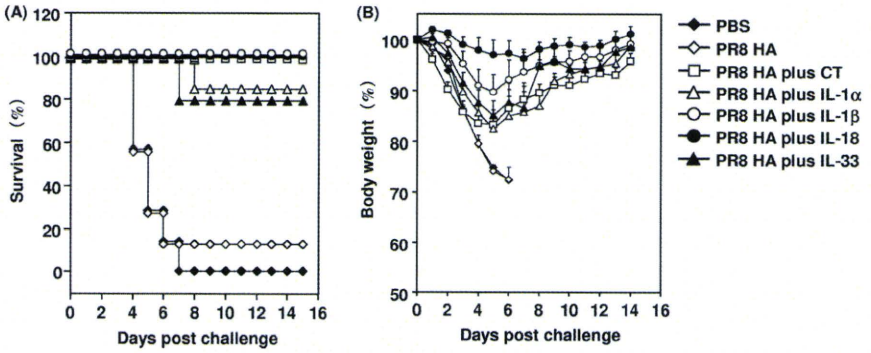

FIG. 6. Protection of BALB/c mice against lethal influenza virus infection by IL-1 family cytokine adjuvants. BALB/c mice were immunized intranasally at 0 and 28 days with rHA alone, rHA plus CT (1 μg/mouse), or rHA plus an IL-1 family cytokine (1 μg/mouse). Fourteen days after the final immunization, mice were intranasally infected with 256 HAU of influenza virus A/PR/8/34. Mice were monitored for survival (A) and weight loss (B) for 14 days after infection. The results are expressed as percent survival (A) and percent initial body weight (B). Data are presented as means ± SEM (n = 4 to 7).

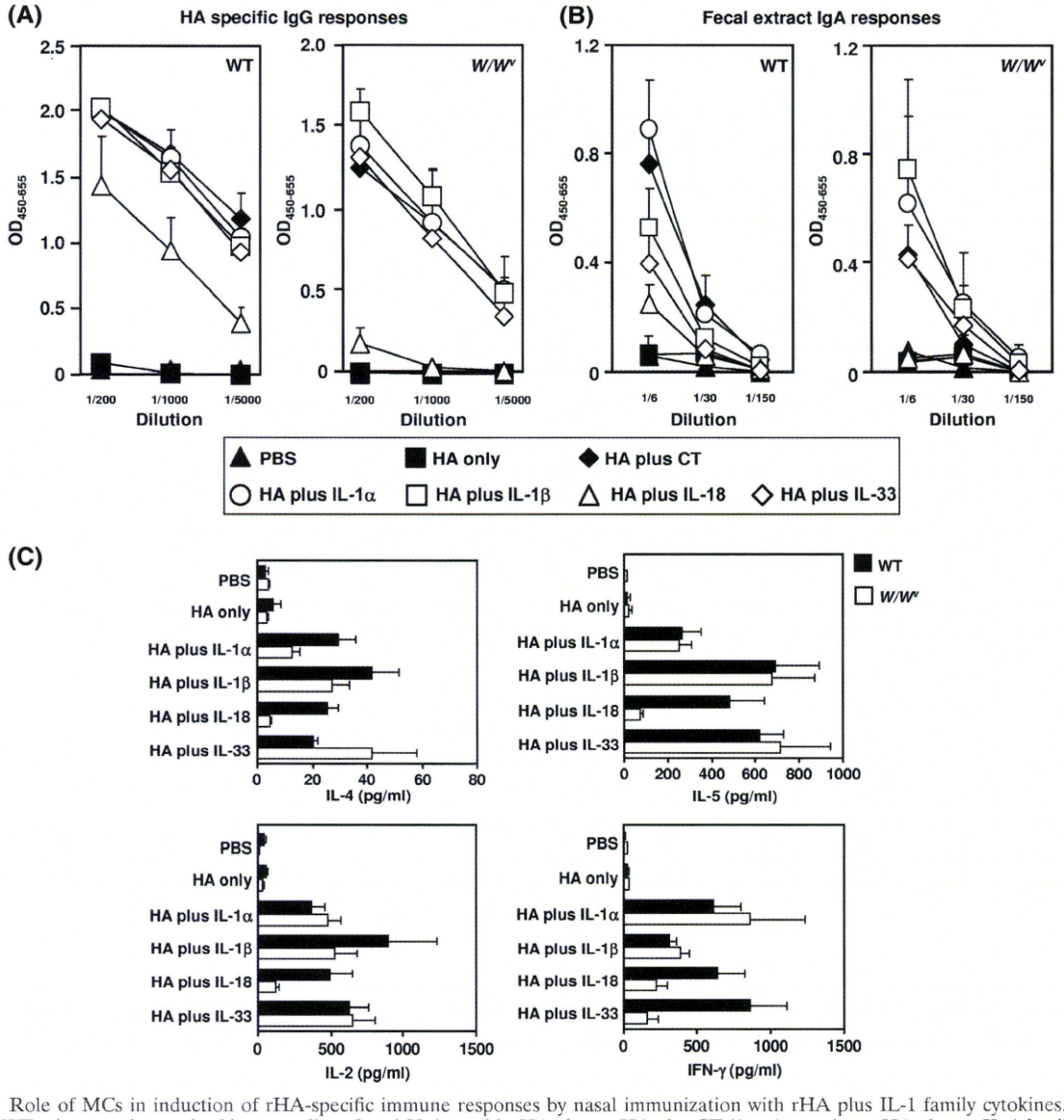

FIG. 7. Role of MCs in induction of rHA-specific immune responses by nasal immunization with rHA plus IL-1 family cytokines. WBB6F1 *W/W*^{v} and WT mice were immunized intranasally at 0 and 28 days with rHA alone, rHA plus CT (1 μg/mouse), or rHA plus an IL-1 family cytokine (1 μg/mouse). Plasma and fecal extracts were collected 14 days after the final immunization and analyzed by ELISA for rHA-specific IgG in plasma (A) and rHA-specific sIgA in fecal extracts (B). (C) Also, 14 days after immunization, splenocytes from each group of WBB6F1 *W/W*^{v} and WT mice were cultured with 10 μg rHA/ml. Culture supernatants were harvested after a 3-day incubation, and rHA-specific cytokine production (IL-4, IL-5, IL-2, and IFN-γ) in the culture supernatants was analyzed using a Bio-Plex multiplex cytokine assay. Data are presented as means ± SEM (n = 5).

IFN-γ-mediated Th1-type immunity in mice immunized with rHA plus IL-33 as a mucosal vaccine adjuvant.

DISCUSSION

Of the 26 different IL cytokines studied here, intranasal immunization with rHA plus an IL-1 family cytokine (IL-1α, IL-1β, IL-18, and IL-33) induced the highest levels of rHA-specific systemic IgG. High levels of sIgA were also observed in the mucosa of IL-1 family cytokine-treated mice. However, IL-12 and IL-15 have been reported to promote systemic and mucosal immunity to intramucosally coadministered protein Ags (8, 45), although more frequent immunization was required to produce adjuvant activity. The apparent discrepancy concerning the adjuvant activity of IL-12 and IL-15 in this study and previous reports may be due to differences in immunization regimens and vaccine doses.

For IL-1 family cytokines, we showed that intranasal administration of rHA plus IL-1α, IL-18, or IL-33 induced higher levels of $CD8^{+}$ CTLs than intranasal administration of rHA alone, whereas the level induced by rHA plus IL-1β was similar to that induced by rHA alone. In agreement with these results, IL-1β has been reported to have a pivotal role in development of Th2-type immune responses (20). A previous report by

Shibuya et al. (36) showed that IL-1α is necessary for optimal Th1 development and IFN-γ secretion in BALB/c mice. In addition, Karupiah et al. (46) showed that IL-18 and IL-12p40 regulate cellular immune responses through $CD8^+$ T-cell activation. Thus, our data are in agreement with previous reports that IL-1α and IL-18 play a pivotal role in inducing Th1-type immune responses. Furthermore, there have been a few reports on the potential of IL-33 to induce a Th1-type immune response (37). In the present study, we showed that of the IL-1 family cytokines, IL-33 induced the highest levels of CTL and IFN-γ^+ cells. We are currently investigating the mechanism of IL-33 in Th1/CTL immunity.

We found that intranasal coadministration of influenza vaccine with IL-1 family cytokines provided protection against influenza viral infection, with IL-1β and IL-18 providing complete protection. It is known that nasal secretions containing locally produced sIgA and serum-derived IgG Abs contribute to forming a first line of defense for combating influenza viral infections (42, 44). Therefore, the prophylactic effects of IL-1 family cytokines may be due mainly to Ab-mediated immunity against influenza virus. Furthermore, previous studies have pointed out the importance of influenza-specific $CD8^+$ CTLs for host recovery from lethal influenza virus infections and protection against further infection (7, 15). Although the mechanism by which IL-18 provided complete protection against influenza remains to be elucidated, high-avidity $CD8^+$ CTLs induced by IL-1α, IL-18, or IL-33 probably confer protection against influenza viral infection. Recently, a requirement for NK cells or NKT cells for control of influenza virus infections was identified (10, 13). Since IL-18 is known to regulate NK and NKT cell activity (4, 38), it is possible that restimulation of these cells may have resulted in the reduction in virus replication and morbidity observed after viral challenge. We are currently investigating the involvement of these cell subsets in the induction of protection against influenza virus by IL-18.

Unfortunately, potent adjuvant action is often correlated with increased toxicity, as exemplified by CT adjuvant, which although it is potent is too toxic for human use. Therefore, one of the major challenges in adjuvant research is to gain potency while minimizing toxicity (17). Intranasal administration of 1 μg of an IL-1 family cytokine for four consecutive days has been shown to induce asthma-like symptoms, including airway hyperresponsiveness and goblet cell hyperplasia in the lungs (26). In contrast, in this study, we found that mice immunized intranasally with IL-1 family cytokines did not exhibit acute toxicity, i.e., there was no cytokine-induced mortality, no obvious weight loss, no abnormal behavior, and no histopathological changes. In addition, use of 0.1 μg of an IL-1 family cytokine as a nasal vaccine adjuvant was still effective at inducing systemic IgG and nasal sIgA Ab responses. Thus, although further safety evaluation is needed, our findings indicate a broad therapeutic utility for IL-1 family cytokines when used as adjuvants for mucosal vaccination.

To develop optimal vaccines for clinical applications, it is important to understand their mechanism of action on the immune system in terms of efficacy as well as safety (23). The present study demonstrates that the enhanced mucosal vaccine adjuvant effect of IL-18 operates via an MC-dependent mechanism. The rHA-specific immune response induced by intranasally administered rHA plus IL-18 in WT mice was significantly reduced in W/W^v mice. In addition, the level of the rHA-specific IFN-γ response in mice intranasally immunized with rHA plus IL-33 was minimal in W/W^v mice. Although studies are needed on the role of MCs in generation of Ag-specific immunity, the studies reported here show that MCs have a role in the effect of IL-18 as an adjuvant and in augmentation of the CTL response induced by IL-33 as a nasal vaccine adjuvant. MC activators (e.g., compound 48/80) have been reported to stimulate protective immune responses against infections (28, 32). In addition, these immune responses are correlated with DC trafficking and lymphocyte recruitment to draining lymph nodes (DLN). Nakae et al. (30) suggested that MC-derived tumor necrosis factor alpha (TNF-α) is required for enhanced recruitment of lymphocytes and DCs to DLN. MC-dependent induction of IL-18 mucosal vaccine adjuvant activity may involve these types of processes. In agreement with this possibility, the IL-18 receptor was highly expressed on the surfaces of MCs but not in nasal passage-associated lymphoid tissue $CD11c^+$ DCs, and IL-18 induced robust TNF-α and IL-6 production from MCs in a concentration-dependent manner *in vitro* (unpublished data). Although further studies are required, IL-18 appeared to exhibit MC-dependent adjuvant activity that was not directly regulated by DC functions, such as DC migration and DC activation.

In summary, IL-1 family cytokines used as mucosal vaccine adjuvants induced two layers of protective immunity when administered intranasally with an influenza virus vaccine Ag, indicating that they may be suitable for use in antiviral nasal vaccines.

ACKNOWLEDGMENTS

We have no financial conflicts of interest.

This study was supported in part by grants-in-aid for scientific research from the Ministry of Education, Culture, Sports, Science and Technology of Japan and from the Japan Society for the Promotion of Science (JSPS). This study was also supported in part by Health Labor Sciences Research Grants from the Ministry of Health, Labor and Welfare of Japan and by Health Sciences Research Grants for Research on Publicly Essential Drugs and Medical Devices from the Japan Health Sciences Foundation.

REFERENCES

1. **Ada, G.** 2001. Vaccines and vaccination. N. Engl. J. Med. **345**:1042–1053.
2. **Ahlers, J. D., I. M. Belyakov, S. Matsui, and J. A. Berzofsky.** 2001. Mechanisms of cytokine synergy essential for vaccine protection against viral challenge. Int. Immunol. **13**:897–908.
3. **Arend, W. P., G. Palmer, and C. Gabay.** 2008. IL-1, IL-18, and IL-33 families of cytokines. Immunol. Rev. **223**:20–38.
4. **Baxevanis, C. N., A. D. Gritzapis, and M. Papamichail.** 2003. In vivo antitumor activity of NKT cells activated by the combination of IL-12 and IL-18. J. Immunol. **171**:2953–2959.
5. **Belyakov, I. M., and J. D. Ahlers.** 2008. Functional CD8+ CTLs in mucosal sites and HIV infection: moving forward toward a mucosal AIDS vaccine. Trends Immunol. **29**:574–585.
6. **Belyakov, I. M., J. D. Ahlers, B. Y. Brandwein, P. Earl, B. L. Kelsall, B. Moss, W. Strober, and J. A. Berzofsky.** 1998. The importance of local mucosal HIV-specific CD8(+) cytotoxic T lymphocytes for resistance to mucosal viral transmission in mice and enhancement of resistance by local administration of IL-12. J. Clin. Invest. **102**:2072–2081.
7. **Bender, B. S., T. Croghan, L. Zhang, and P. A. Small, Jr.** 1992. Transgenic mice lacking class I major histocompatibility complex-restricted T cells have delayed viral clearance and increased mortality after influenza virus challenge. J. Exp. Med. **175**:1143–1145.
8. **Boyaka, P. N., M. Marinaro, R. J. Jackson, S. Menon, H. Kiyono, E. Jirillo, and J. R. McGhee.** 1999. IL-12 is an effective adjuvant for induction of mucosal immunity. J. Immunol. **162**:122–128.

9. **Boyaka, P. N., M. Ohmura, K. Fujihashi, T. Koga, M. Yamamoto, M. N. Kweon, Y. Takeda, R. J. Jackson, H. Kiyono, Y. Yuki, and J. R. McGhee.** 2003. Chimeras of labile toxin one and cholera toxin retain mucosal adjuvanticity and direct Th cell subsets via their B subunit. J. Immunol. **170:**454–462.
10. **Cerwenka, A., and L. L. Lanier.** 2001. Natural killer cells, viruses and cancer. Nat. Rev. Immunol. **1:**41–49.
11. **Croft, M.** 2009. The role of TNF superfamily members in T-cell function and diseases. Nat. Rev. Immunol. **9:**271–285.
12. **De Gregorio, E., U. D'Oro, and A. Wack.** 2009. Immunology of TLR-independent vaccine adjuvants. Curr. Opin. Immunol. **21:**339–345.
13. **Diana, J., and A. Lehuen.** 2009. NKT cells: friend or foe during viral infections? Eur. J. Immunol. **39:**3283–3291.
14. **Dinarello, C. A.** 2009. Immunological and inflammatory functions of the interleukin-1 family. Annu. Rev. Immunol. **27:**519–550.
15. **Doherty, P. C., J. M. Riberdy, and G. T. Belz.** 2000. Quantitative analysis of the CD8+ T-cell response to readily eliminated and persistent viruses. Philos. Trans. R. Soc. Lond. B Biol. Sci. **355:**1093–1101.
16. **Galli, S. J., S. Nakae, and M. Tsai.** 2005. Mast cells in the development of adaptive immune responses. Nat. Immunol. **6:**135–142.
17. **Griffin, M. R., M. M. Braun, and K. J. Bart.** 2009. What should an ideal vaccine postlicensure safety system be? Am. J. Public Health **99**(Suppl. 2)**:**S345–S350.
18. **Haynes, B. F., and R. J. Shattock.** 2008. Critical issues in mucosal immunity for HIV-1 vaccine development. J. Allergy Clin. Immunol. **122:**3–9.
19. **Heib, V., M. Becker, T. Warger, G. Rechtsteiner, C. Tertilt, M. Klein, T. Bopp, C. Taube, H. Schild, E. Schmitt, and M. Stassen.** 2007. Mast cells are crucial for early inflammation, migration of Langerhans cells, and CTL responses following topical application of TLR7 ligand in mice. Blood **110:** 946–953.
20. **Helmby, H., and R. K. Grencis.** 2004. Interleukin 1 plays a major role in the development of Th2-mediated immunity. Eur. J. Immunol. **34:**3674–3681.
21. **Holmgren, J., and C. Czerkinsky.** 2005. Mucosal immunity and vaccines. Nat. Med. **11:**S45–S53.
22. **Hubbell, J. A., S. N. Thomas, and M. A. Swartz.** 2009. Materials engineering for immunomodulation. Nature **462:**449–460.
23. **Ishii, K. J., T. Kawagoe, S. Koyama, K. Matsui, H. Kumar, T. Kawai, S. Uematsu, O. Takeuchi, F. Takeshita, C. Coban, and S. Akira.** 2008. TANK-binding kinase-1 delineates innate and adaptive immune responses to DNA vaccines. Nature **451:**725–729.
24. **Kayamuro, H., Y. Abe, Y. Yoshioka, K. Katayama, T. Nomura, T. Yoshida, K. Yamashita, T. Yoshikawa, Y. Kawai, T. Mayumi, T. Hiroi, N. Itoh, K. Nagano, H. Kamada, S. Tsunoda, and Y. Tsutsumi.** 2009. The use of a mutant TNF-alpha as a vaccine adjuvant for the induction of mucosal immune responses. Biomaterials **30:**5869–5876.
25. **Kayamuro, H., Y. Yoshioka, Y. Abe, K. Katayama, T. Yoshida, K. Yamashita, T. Yoshikawa, T. Hiroi, N. Itoh, Y. Kawai, T. Mayumi, H. Kamada, S. Tsunoda, and Y. Tsutsumi.** 2009. TNF superfamily member, TL1A, is a potential mucosal vaccine adjuvant. Biochem. Biophys. Res. Commun. **384:** 296–300.
26. **Kondo, Y., T. Yoshimoto, K. Yasuda, S. Futatsugi-Yumikura, M. Morimoto, N. Hayashi, T. Hoshino, J. Fujimoto, and K. Nakanishi.** 2008. Administration of IL-33 induces airway hyperresponsiveness and goblet cell hyperplasia in the lungs in the absence of adaptive immune system. Int. Immunol. **20:**791–800.
27. **Marinaro, M., H. F. Staats, T. Hiroi, R. J. Jackson, M. Coste, P. N. Boyaka, N. Okahashi, M. Yamamoto, H. Kiyono, H. Bluethmann, K. Fujihashi, and J. R. McGhee.** 1995. Mucosal adjuvant effect of cholera toxin in mice results from induction of T helper 2 (Th2) cells and IL-4. J. Immunol. **155:**4621–4629.
28. **McLachlan, J. B., C. P. Shelburne, J. P. Hart, S. V. Pizzo, R. Goyal, R. Brooking-Dixon, H. F. Staats, and S. N. Abraham.** 2008. Mast cell activators: a new class of highly effective vaccine adjuvants. Nat. Med. **14:**536–541.
29. **Mutsch, M., W. Zhou, P. Rhodes, M. Bopp, R. T. Chen, T. Linder, C. Spyr, and R. Steffen.** 2004. Use of the inactivated intranasal influenza vaccine and the risk of Bell's palsy in Switzerland. N. Engl. J. Med. **350:**896–903.
30. **Nakae, S., H. Suto, M. Kakurai, J. D. Sedgwick, M. Tsai, and S. J. Galli.** 2005. Mast cells enhance T cell activation: importance of mast cell-derived TNF. Proc. Natl. Acad. Sci. U. S. A. **102:**6467–6472.
31. **Neutra, M. R., and P. A. Kozlowski.** 2006. Mucosal vaccines: the promise and the challenge. Nat. Rev. Immunol. **6:**148–158.
32. **Pulendran, B., and S. J. Ono.** 2008. A shot in the arm for mast cells. Nat. Med. **14:**489–490.
33. **Reddy, S. T., M. A. Swartz, and J. A. Hubbell.** 2006. Targeting dendritic cells with biomaterials: developing the next generation of vaccines. Trends Immunol. **27:**573–579.
34. **Reed, S. G., S. Bertholet, R. N. Coler, and M. Friede.** 2009. New horizons in adjuvants for vaccine development. Trends Immunol. **30:**23–32.
35. **Sasaki, Y., T. Yoshimoto, H. Maruyama, T. Tegoshi, N. Ohta, N. Arizono, and K. Nakanishi.** 2005. IL-18 with IL-2 protects against Strongyloides venezuelensis infection by activating mucosal mast cell-dependent type 2 innate immunity. J. Exp. Med. **202:**607–616.
36. **Shibuya, K., D. Robinson, F. Zonin, S. B. Hartley, S. E. Macatonia, C. Somoza, C. A. Hunter, K. M. Murphy, and A. O'Garra.** 1998. IL-1 alpha and TNF-alpha are required for IL-12-induced development of Th1 cells producing high levels of IFN-gamma in BALB/c but not C57BL/6 mice. J. Immunol. **160:**1708–1716.
37. **Smithgall, M. D., M. R. Comeau, B. R. Yoon, D. Kaufman, R. Armitage, and D. E. Smith.** 2008. IL-33 amplifies both Th1- and Th2-type responses through its activity on human basophils, allergen-reactive Th2 cells, iNKT and NK cells. Int. Immunol. **20:**1019–1030.
38. **Son, Y. I., R. M. Dallal, R. B. Mailliard, S. Egawa, Z. L. Jonak, and M. T. Lotze.** 2001. Interleukin-18 (IL-18) synergizes with IL-2 to enhance cytotoxicity, interferon-gamma production, and expansion of natural killer cells. Cancer Res. **61:**884–888.
39. **Spangler, B. D.** 1992. Structure and function of cholera toxin and the related Escherichia coli heat-labile enterotoxin. Microbiol. Rev. **56:**622–647.
40. **Stelekati, E., R. Bahri, O. D'Orlando, Z. Orinska, H. W. Mittrucker, R. Langenhaun, M. Glatzel, A. Bollinger, R. Paus, and S. Bulfone-Paus.** 2009. Mast cell-mediated antigen presentation regulates CD8+ T cell effector functions. Immunity **31:**665–676.
41. **Surh, C. D., and J. Sprent.** 2008. Homeostasis of naive and memory T cells. Immunity **29:**848–862.
42. **Tamura, S., Y. Ito, H. Asanuma, Y. Hirabayashi, Y. Suzuki, T. Nagamine, C. Aizawa, and T. Kurata.** 1992. Cross-protection against influenza virus infection afforded by trivalent inactivated vaccines inoculated intranasally with cholera toxin B subunit. J. Immunol. **149:**981–988.
43. **Toka, F. N., C. D. Pack, and B. T. Rouse.** 2004. Molecular adjuvants for mucosal immunity. Immunol. Rev. **199:**100–112.
44. **Tumpey, T. M., M. Renshaw, J. D. Clements, and J. M. Katz.** 2001. Mucosal delivery of inactivated influenza vaccine induces B-cell-dependent heterosubtypic cross-protection against lethal influenza A H5N1 virus infection. J. Virol. **75:**5141–5150.
45. **Wang, X., X. Zhang, Y. Kang, H. Jin, X. Du, G. Zhao, Y. Yu, J. Li, B. Su, C. Huang, and B. Wang.** 2008. Interleukin-15 enhance DNA vaccine elicited mucosal and systemic immunity against foot and mouth disease virus. Vaccine **26:**5135–5144.
46. **Wang, Y., G. Chaudhri, R. J. Jackson, and G. Karupiah.** 2009. IL-12p40 and IL-18 play pivotal roles in orchestrating the cell-mediated immune response to a poxvirus infection. J. Immunol. **183:**3324–3331.

Solution of the Structure of the TNF-TNFR2 Complex

Yohei Mukai, Teruya Nakamura, Mai Yoshikawa, Yasuo Yoshioka, Shin-ichi Tsunoda, Shinsaku Nakagawa, Yuriko Yamagata and Yasuo Tsutsumi (16 November 2010)

Science Signaling **3** (148), ra83. [DOI: 10.1126/scisignal.2000954]

BIOCHEMISTRY

Solution of the Structure of the TNF-TNFR2 Complex

Yohei Mukai,[1,2*] Teruya Nakamura,[3] Mai Yoshikawa,[1,2] Yasuo Yoshioka,[1,2,4] Shin-ichi Tsunoda,[1,4,5*] Shinsaku Nakagawa,[2] Yuriko Yamagata,[3] Yasuo Tsutsumi[1,4,6*]

(Published 16 November 2010; Volume 3 Issue 148 ra83)

Tumor necrosis factor (TNF) is an inflammatory cytokine that has important roles in various immune responses, which are mediated through its two receptors, TNF receptor 1 (TNFR1) and TNFR2. Antibody-based therapy against TNF is used clinically to treat several chronic autoimmune diseases; however, such treatment sometimes results in serious side effects, which are thought to be caused by the blocking of signals from both TNFRs. Therefore, knowledge of the structural basis for the recognition of TNF by each receptor would be invaluable in designing TNFR-selective drugs. Here, we solved the 3.0 angstrom resolution structure of the TNF-TNFR2 complex, which provided insight into the molecular recognition of TNF by TNFR2. Comparison to the known TNFR1 structure highlighted several differences between the ligand-binding interfaces of the two receptors. Additionally, we also demonstrated that TNF-TNFR2 formed aggregates on the surface of cells, which may be required for signal initiation. These results may contribute to the design of therapeutics for autoimmune diseases.

INTRODUCTION

Tumor necrosis factor (TNF) is an immunity-modulating cytokine that is required for defense against infectious diseases and carcinogenesis (*1*). Excess amounts of TNF, however, cause various autoimmune diseases, such as rheumatoid arthritis (RA), Crohn's disease, and ulcerative colitis (*2*–*4*). TNF activates signals through its two receptors [the type I TNF receptor (TNFR1) and TNFR2], and these molecules are well-known targets in therapies against autoimmune diseases (*1*, *5*). Currently, TNF neutralization therapies through the use of a soluble TNFR2-Fc chimera (etanercept), a mouse-human chimera monoclonal antibody against TNF (infliximab), or a fully humanized monoclonal antibody against TNF (adalimumab) have proven to be effective treatments for RA (*6*, *7*). Unfortunately, however, a block of TNF-mediated host defense often increases the risk of bacterial or viral infection (*8*, *9*) or of the development of lymphoma (*10*). Thus, a thorough understanding of the function of the TNF-TNFR complex is important for the design of optimal therapies against the various TNF-related autoimmune diseases.

TNFR1 and TNFR2 activate distinct cell signaling pathways. TNFR1 is ubiquitously expressed, whereas TNFR2 is found mostly on certain populations of immune cells. In general, TNFR1 is largely associated with the apoptotic activity of TNF, whereas TNFR2 is involved in T cell survival (*11*). Thus, both proteins must be fully analyzed to better understand the function of TNF. Previous studies with animal models of diseases such as arthritis and hepatitis demonstrated the predominant role of TNFR1 in the pathogenesis and exacerbation of inflammation (*12*, *13*). Nonetheless, TNFR2 is crucial for antigen-stimulated activation and proliferation of T cells (*14*–*16*), which is essential for cell-mediated immunity to pathogens. In addition, transmembrane TNF (tmTNF), the prime activating ligand of TNFR2 (*17*), is sufficient to control infection by *Mycobacterium tuberculosis* (*18*, *19*), indicating the importance of TNFR2 in this type of bacterial infection. Other reports showed that TNFR2 is important in the function of regulatory T cells (*20*), suggesting a role for tmTNF-TNFR2 signaling in anti-inflammatory effects. On the basis of these studies, the specific blocking of TNFR1 signaling appears to be a promising approach to minimize the side effects that are associated with "anti-TNF" therapy (*5*, *11*, *21*, *22*). Thus, it is highly desirable to establish a structural basis for the differences between TNFR1 and TNFR2.

One structural characteristic shared by most members of the TNFR superfamily is that they contain from about two to four cysteine-rich domains (CRDs) (*5*). The first structure of a TNFR superfamily member to be determined was the crystal structure of the lymphotoxin-α (LT-α)–TNFR1 complex (*23*). The authors of that study suggested that the protein fold is characterized by multiple disulfide linkages in the CRD and that these bonds are important in stabilizing the structure of the TNFR. Moreover, a trimer of LT-α binds to three TNFR1 monomers through CRD2 and CRD3 in TNFR1, suggesting that trimerization of TNFRs is directly related to their signaling. The structural similarity between TNF and LT-α suggests that TNF should be able to form a complex with TNFR1 that resembles that of LT-α–TNFR1 (*23*–*25*). More recently, the structures of complexes of other TNF-TNFR superfamily proteins have been solved, including TNF-related apoptosis-inducing ligand (TRAIL)–death receptor 5 (DR5) (*26*–*28*) and CD134 antigen (OX40) ligand (OX40L)–OX40 (*29*). These reports suggest that the structural features that were described for the LT-α–TNFR1 complex are common to other TNF-TNFR superfamily members. Moreover, a study revealed the crystal structure of TNF in a complex with a viral TNF inhibitor (poxvirus 2L protein) (*30*) that is important for viral escape from TNF-mediated immunity (*31*). Therefore, determination of the structure of TNFR2 and of its role in immunity against pathogens would be useful in understanding the details of basic TNF functions.

[1]Laboratory of Biopharmaceutical Research, National Institute of Biomedical Innovation, Osaka 567-0085, Japan. [2]Department of Biotechnology and Therapeutics, Graduate School of Pharmaceutical Sciences, Osaka University, Osaka 565-0871, Japan. [3]Graduate School of Pharmaceutical Sciences, Kumamoto University, Kumamoto 862-0973, Japan. [4]Center for Advanced Medical Engineering and Informatics, Osaka University, 1-6 Yamadaoka, Suita, Osaka 565-0871, Japan. [5]Department of Biomedical Innovation, Graduate School of Pharmaceutical Sciences, Osaka University, Osaka 565-0871, Japan. [6]Department of Toxicology and Safety Science, Graduate School of Pharmaceutical Sciences, Osaka University, Osaka 565-0871, Japan.
*To whom correspondence should be addressed. E-mail: yohe@phs.osaka-u.ac.jp (Y.M.); tsunoda@nibio.go.jp (S.T.); ytsutsumi@phs.osaka-u.ac.jp (Y.T.).

Another important characteristic of the TNFR superfamily is that many of these proteins exist as preassembled oligomers on the cell surface [for example, Fas (Apo-1/CD95), TNFR1, and TNFR2] (*32*, *33*). This ligand-independent assembly of TNFR oligomers is mediated by the preligand assembly domain (PLAD), which resides within the N-terminal CRD (CRD1) of the TNFRs and is not directly involved in binding to ligand (*33*). PLAD-mediated, ligand-independent assembly has also been reported for TRAIL receptors and viral homologs of TNFR (*34*, *35*). Ligand-independent assembly of receptors was reported for other cytokine members, such as the interleukin-17 receptor (*36*), which indicates that this phenomenon is important for various immune responses. Indeed, the PLAD of TNFRs is critical for TNF-mediated responses (*33*), and soluble PLAD can effectively prevent TNFR signaling and potently inhibit inflammatory arthritis (*37*). These results suggest that PLAD-mediated receptor assembly is essential for TNFR signaling. However, in the crystal structures of other TNF-TNFR superfamily complexes, such as TNFR1, DR5, and OX40, individual PLADs are disassociated (*23*, *26*–*29*). This apparent contradiction regarding PLAD-mediated receptor assembly must be resolved to understand the molecular basis for TNFR-mediated signal initiation. We reasoned that the behavior of the TNF-TNFR complex on the surface of live cells needed to be investigated to understand the molecular basis of the ligand-receptor interactions.

Here, we determined the first crystal structure of the TNF-TNFR2 complex. With these data, we analyzed the structural basis for how TNF can bind to two divergent receptors (TNFR1 and TNFR2) of the same superfamily. This finding contributes to an understanding of the differences between TNFR1 and TNFR2, which may be useful for rationalizing selectivity data and for generating hypotheses to design future TNFR-selective drugs (*11*, *21*). Finally, we discuss the signal initiation mechanism of the TNFR superfamily by analyzing the behavior of the preassembled TNFR2 and TNF-TNFR2 complexes on the surface of a live cell. This is the first report to describe the structural details of a TNF-TNFR2 complex in a crystal and in cells. These findings contribute to our knowledge of members of the TNF superfamily and may provide a new focus for investigation of the signaling machinery of cell surface receptors.

Table 1. Refinement statistics of the TNF-TNFR2 crystal. Ramachandran statistics indicate the fraction of residues in the favored, allowed, and outlier region, respectively, of the Ramachandran diagram as defined by the RAMPAGE program (*65*).

Refinement statistics	
Resolution (Å)	49.96–3.00
Reflections used	43,981
R_{cryst} (%)*	21.3
R_{free} (%)†	28.1
Completeness (%)	99.5
Atoms	
Protein	13,922
Water	11
Co^{2+}	6
RMSD in bonds (Å)	0.004
RMSD in angles (°)	0.759
Ramachandran plot	
Favored region (%)	92.9
Allowed region (%)	6.5
Outlier region (%)	0.6

*$R_{cryst} = \Sigma||F_{obs}| - |F_{calc}||/\Sigma|F_{obs}|$, where F_{obs} and F_{calc} are the observed and calculated structure factors, respectively. †R_{free} is calculated as for R_{cryst}, but for the test set that consists of reflections not used in refinement.

RESULTS

Determination of the structure of the TNF-TNFR2 complex

In a previous report, we obtained a crystal of the TNF-TNFR2 complex belonging to the space group $P2_12_12_1$, as well as preliminary x-ray diffraction data to 2.95 Å (*38*). Here, we solved the structure of the TNF-TNFR2 complex by molecular replacement with the crystal structure of another TNF mutant that we described previously [Protein Data Bank (PDB) code 2e7a] (*39*). Diffraction data sets at 3.0 Å were used in refinements, and the final *R*-factor was 21.3% (with a free *R*-factor of 28.1%) (Table 1). Although we used mutTNF Lys (−) (a lysine-deficient mutant of human TNF that is fully active) (*40*) as the TNF molecule in the TNF-TNFR2 complex (*38*), it was confirmed that mutTNF Lys (−) in the TNF-TNFR2 complex retained almost the same structure as that of wild-type TNF [root mean square deviations (RMSDs) of 0.94 Å for 420 Cα atoms].

We found that the asymmetric unit in the crystal contained two copies of the TNF-TNFR2 complex, which formed an interlocking dimer (two trimers of TNF and six monomers of TNFR2) (Fig. 1, A and B). In this interlocking dimer, CRD2-CRD4 interactions were mainly observed between opposite TNFR2 molecules (Fig. 1, C and D). We observed a potential intermolecular hydrogen bond between Asp^{81} in CRD2 and the amido NH group near Thr^{151} in CRD4 (Fig. 1, E and F), but each TNFR2 mainly interacted through van der Waals contacts. The buried surface area of this interface was relatively extensive (~4300 $Å^2$ for every two copies of the complex), in contrast to ~2500 $Å^2$ in the high-affinity TNF-TNFR2 binding interface. However, according to analytical gel-filtration experiments, the purified TNF-TNFR2 complex in aqueous solution is 110 kD (*38*), which suggests that the TNF-TNFR2 complex contains one trimer of TNF (51 kD) and three monomers of TNFR2 (19 kD each) in aqueous solution. Moreover, the position of the C terminus of TNFR2 suggested that this interlocking dimer would be difficult to form on the cell surface (Fig. 1C). Therefore, we suggested that the formation of such interlocking dimers was a result of crystal packing.

Nonetheless, previous studies showed that mutation of Met^{174} of TNFR2 to Arg, which is referred to as the "M196R polymorphism," is associated with the presence of soluble TNFR2 in the serum (*41*) and autoimmune diseases, such as systemic lupus erythematosus (*42*, *43*). The crystal packing of TNFR2 showed that Met^{174} was located near Arg^{77} of other TNFR2 molecules (Fig. 1, E and F), which suggests that the mutant Arg^{174} residue influences the interaction between the CRD2 of one TNFR2 molecule and the CRD4 of another TNFR2 molecule in the crystal. Although previous gel-filtration analysis suggested that this interlocking dimer was formed by crystal packing, the report on the mutation of Met^{174} in TNFR2 suggests that the interlocking dimer might form only under the specific condition in which TNFR2 is soluble.

TNFR2 structure

The structures of the extracellular domains of members of the TNFR superfamily are composed of CRDs that typically contain six cysteine residues that form three disulfide bonds (*23*). TNFR1 and TNFR2 contain four CRDs, termed CRD1 through CRD4 (Fig. 2A). CRD1 (also known as PLAD) is essential for forming the TNFR self-complex on the cell surface (*33*). CRD2 and CRD3 are known as TNF-binding domains (*23*), whereas the function of CRD4 remains unclear.

Through comparison of the structures of TNFR2 and TNFR1, together with alignment of their corresponding sequences, we found that CRD1 and CRD2 were topologically and structurally similar in both receptors (Fig. 2B). These CRDs contained the modules A1 and B2, which are typically observed in conventional members of the TNFR superfamily (*44*),

such as the structurally determined TNFR1 (*23*), DR5 (*26–28*), and OX40 (*29*) proteins. The A1 module contains a single disulfide bond, whereas the B2 module contains two disulfides, in a consensus sequence pattern. Of note, and different from the CRD3 of TNFR1, the CRD3 of TNFR2 contained the A2 module that is observed in a certain type of TNFR superfamily members, such as the CD30, CD40, and 4-1BB proteins (*44*). Because these TNFR superfamily members have not been structurally identified yet, our structure of the TNF-TNFR2 complex is the first to show the structure of the A2 module. The A2 module in TNFR2 contained two disulfides that were linked in a 1-4, 2-3 topology (Fig. 2C). The 2-3 disulfide (between Cys^{104} and Cys^{112}) contributed to deflect a β-turn motif that was near the ligand-binding region (Fig. 2D), similar to the structure predicted from the A2 module in a viral protein homologous to TNFR2 (*45*). As a result of this disulfide bond, a gap between CRD2 and CRD3 in TNFR2 was buried in the structure (region 1 in Fig. 2, D and E). The location of Arg^{77} in the CRD2 of TNFR1, which is thought to be essential for binding to TNF (*23*), was compensated by Arg^{113} of the TNFR2 CRD3 in the TNF-TNFR2 structure. This structural difference between TNFR1 and TNFR2 was thought to depend on the diversity of their modules.

We observed another structural difference between TNFR1 and TNFR2 in region 2 (Fig. 2, D and E). A loop structure in TNFR1, which is reported to constitute the ligand-binding region (*23*), consisted of five residues in TNFR1 (Arg^{77} to Gly^{81}) but only three residues in TNFR2 (Ser^{79} to Asp^{81}) (Fig. 2B). The shorter loop structure of TNFR2 was further from the molecular surface of TNF ligand compared with that of TNFR1 as described below.

The TNF-TNFR2 complex

We found that TNF formed a central homotrimer around which three TNFR2 molecules were bound, similar to the known structures of other TNF superfamily members, including LT-α–TNFR1 (*23*), TRAIL-DR5 (*26–28*), and OX40L-OX40 (*29*) (Fig. 3, A and B). The structure of the TNF-TNFR2 complex revealed that the TNFR1-binding region of TNF overlapped with its TNFR2-binding region, as previously predicted (*46*). One TNFR2 molecule interacted with two TNF molecules, as is the case for the LT-α–TNFR1 complex. The core of the interface between TNFR2 and TNF was separated into two regions, termed regions 3 and 4 (Fig. 3, B to D). Region 3 consisted of the A1 module of CRD2, whereas region 4, which was near regions 1 and 2, consisted of the B2 module of CRD2 and the A2 module of CRD3. Comparison of the electrostatic surface potentials of TNFR1 and TNFR2 showed that they were different despite sharing the same binding partner (Fig. 3, C and D). In the interface of TNFR2 region 3, acidic amino acid residues (Asp^{54}, Glu^{57}, and Glu^{70}) were clustered, forming a more negatively charged surface than that of TNFR1. Moreover, in region 4 of TNFR2, the molecular surface was different from that of TNFR1, possibly as a result of diversity in the modules present (Fig. 2B). This structural feature contributed to the exposure of basic amino acids (Arg^{77}, Lys^{108}, and Arg^{133}) at the binding interface, which generated a positively charged surface on TNFR2.

Although a cobalt ion (Co^{2+}) from the crystallization reagent was observed at all six interfaces in the asymmetric unit (Fig. 4A), Arg^{31} of TNF appeared to interact with the negatively charged region 3 on the surface of TNFR2 (Fig. 4B). By contrast, our model of the TNF-TNFR1 complex, constructed from the structure of the LT-α–TNFR1 complex, indicated that the interaction between Arg^{31} and the TNFR1 might be weak, because of the neutral charge of region 3 (Fig. 4C). Indeed, a previously reported R31D mutant of TNF displays a marked loss of affinity for TNFR2 while retaining affinity for TNFR1 (*47*). Therefore, these results suggest that this electrostatic interaction between Arg^{31} of TNF and TNFR is more important for the TNF-TNFR2 complex than for that of TNF and TNFR1. We found that Arg^{32} of TNF was located in a position that enabled a potential hydrogen bond to be formed with Ser^{73} of TNFR2 and that it seemed to interact with Ser^{72} of TNFR1 in the same way. Therefore, we suggest that Arg^{32} of TNF contributes equally to the binding of TNF to TNFR1 and TNFR2.

Detail of region 4 showed that Arg^{113} and Arg^{77} of TNFR2 formed close contacts to Asp^{143}, Gln^{149}, and Glu^{23} of TNF, potentially through the formation of hydrogen bonds. Thus, Arg^{113} and Arg^{77} of TNFR2 were important residues for binding to TNF (Fig. 4, E and F). This result is also supported from previous analysis of point mutations of TNF (*46*, *48*, *49*). Meanwhile, Arg^{77} of TNFR1 appeared to interact with Asp^{143} and Gln^{149} of TNF (Fig. 4F). We suggest that Arg^{113} of TNFR2 and Arg^{77} of TNFR1 might have similar roles in binding to TNF (Fig. 4, E and F). This difference regarding arginine residues between TNFR1 and TNFR2 was also indicated earlier (Fig. 2, D and E). The origin of this difference in inter-

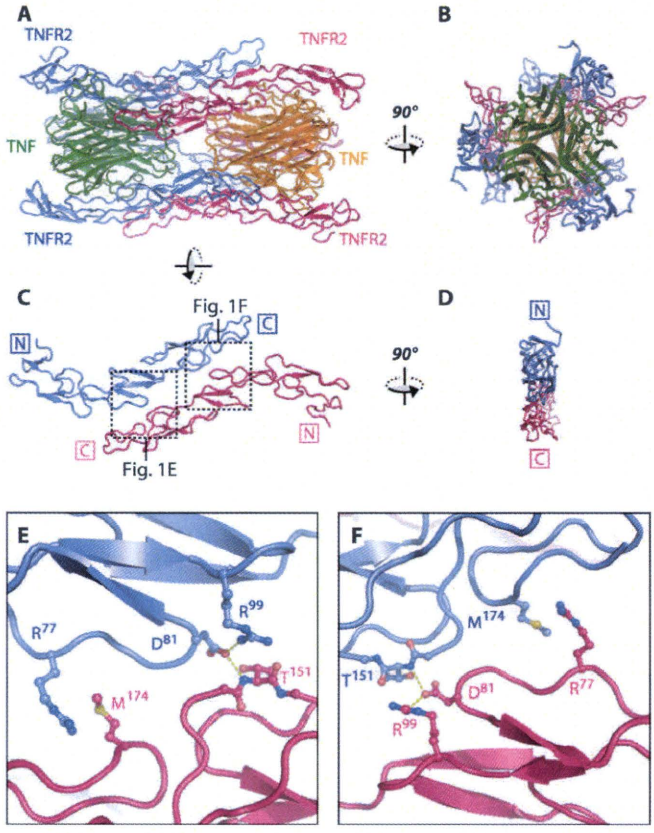

Fig. 1. TNF-TNFR2 complex in the asymmetric unit. Two TNF-TNFR2 complexes are observed in the asymmetric unit (consisting of two TNF trimers and six TNFR2 monomers). TNFR2 molecules from different complexes interact with each other in the crystal. TNF molecules are shown in green and orange; TNFR2 molecules are shown in blue and red. (**A** and **B**) Side view (A) and top view (B) of the complexes. (**C** and **D**) Side view (C) and top view (D) of the TNFR2-TNFR2 interaction in the crystal. N, N terminus; C, C terminus. (**E** and **F**) Details of the TNFR2-TNFR2 interfaces. Close contacts that are suggestive of potential hydrogen bonds are shown as yellow dashed lines.

action was a result of the unique A2 module and the dynamic structural diversity close to regions 1, 2, and 4.

Usefulness of the molecular pocket formulation for the design of TNFR1-selective inhibitors

Differences in the composition of the respective modules together with the diversity in the length of the main chain near the binding interface constitute the basic structural elements that distinguish TNFR1 from TNFR2. These structural considerations could form the basis of the design of receptor-specific drugs. Previous mutational analysis showed that region 1 of TNFR1 and TNFR2 (Fig. 2, D and E) is essential for the interaction with the loop of TNF (amino acid residues 143 to 149) (*46*, *48*, *49*). In this ligand-binding area of TNFR2, the turn motif of CRD3 (Ser^{107} to Cys^{112}) fit to its CRD2 in the presence of the disulfide bond between Cys^{104} and Cys^{112} (Figs. 2D and 5A). By contrast, there was a space between the turn motif of the CRD3 of TNFR1 and the β strand of its CRD2, which resulted in the formation of a molecular pocket specifically on the surface of TNFR1 (Fig. 5B). These observations suggest that this region of TNFR1 constitutes a promising target for the structure-based development of TNFR1-selective drugs.

Another point of interest was observed in region 2. A number of amino acid residues contained in the loop structure of region 2 differ between TNFR1 and TNFR2 (Fig. 2B). In the shorter loop of TNFR2 (residues Ser^{79} to Asp^{81}), there was a space between TNF and the receptor

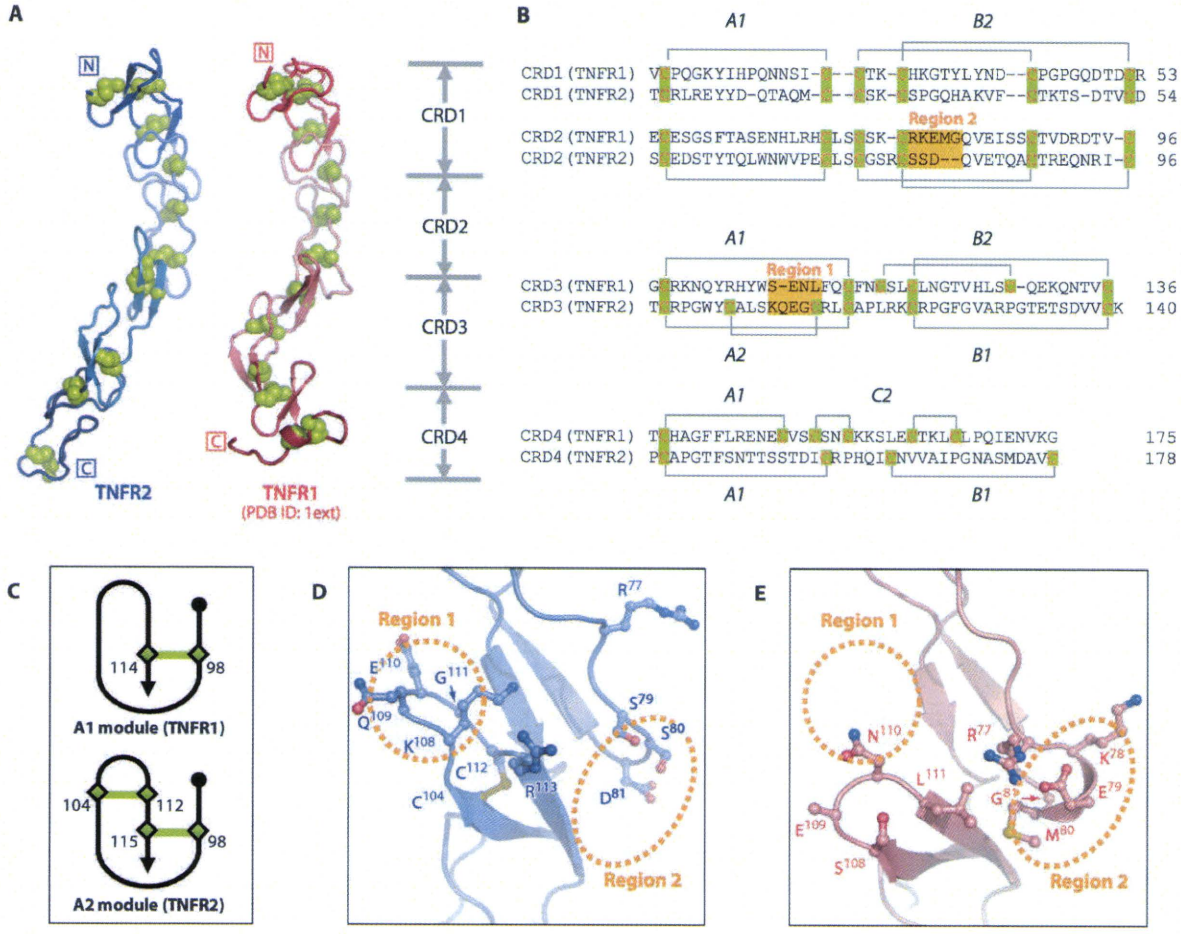

Fig. 2. Basic structure and folding of TNFR2 and TNFR1. (**A**) Structure of the extracellular domain of TNFR2 in blue (PDB ID 3alq) and TNFR1 in red (PDB ID 1ext). Disulfide linkages are shown as green spheres. For a comparison of the basic structures, we superimposed a crystal structure of unbound TNFR1 (CRD1 to CRD3 of PDB ID 1ext) (*55*) onto the structure of TNFR2 (CRD1 to CRD3) with the SUPERPOSE program (*67*) in CCP4i. (**B**) Alignment of the amino acid sequences of TNFR1 and TNFR2. A1, A2, B1, B2, and C2 are the names of the module structures. Cysteine residues are highlighted in green. Differences between the structures of TNFR1 and TNFR2 (regions 1 and 2) are highlighted in orange. The amino acid sequence alignment was performed with the ClustalW program (*68*). Abbreviations for the amino acids are as follows: A, Ala; C, Cys; D, Asp; E, Glu; F, Phe; G, Gly; H, His; I, Ile; K, Lys; L, Leu; M, Met; N, Asn; P, Pro; Q, Gln; R, Arg; S, Ser; T, Thr; V, Val; W, Trp; and Y, Tyr. (**C**) The A1 and A3 modules. There are different modules in the CRD3 regions of TNFR1 and TNFR2. (**D**) Ligand-binding interface of TNFR2. (**E**) Receptor binding interface of TNFR1. To compare the binding interfaces, we superimposed a crystal structure of TNFR1 complexed with LT-α (CRD1 to CRD3 of PDB ID 1tnr) onto the structure of TNFR2 (CRD1 to CRD3) with the SUPERPOSE program. The side chain of Glu^{109} is missing in the structure of TNFR1 (PDB ID 1tnr). Structural differences between TNFR1 and TNFR2 (regions 1 and 2) are also highlighted by orange dashed circles.

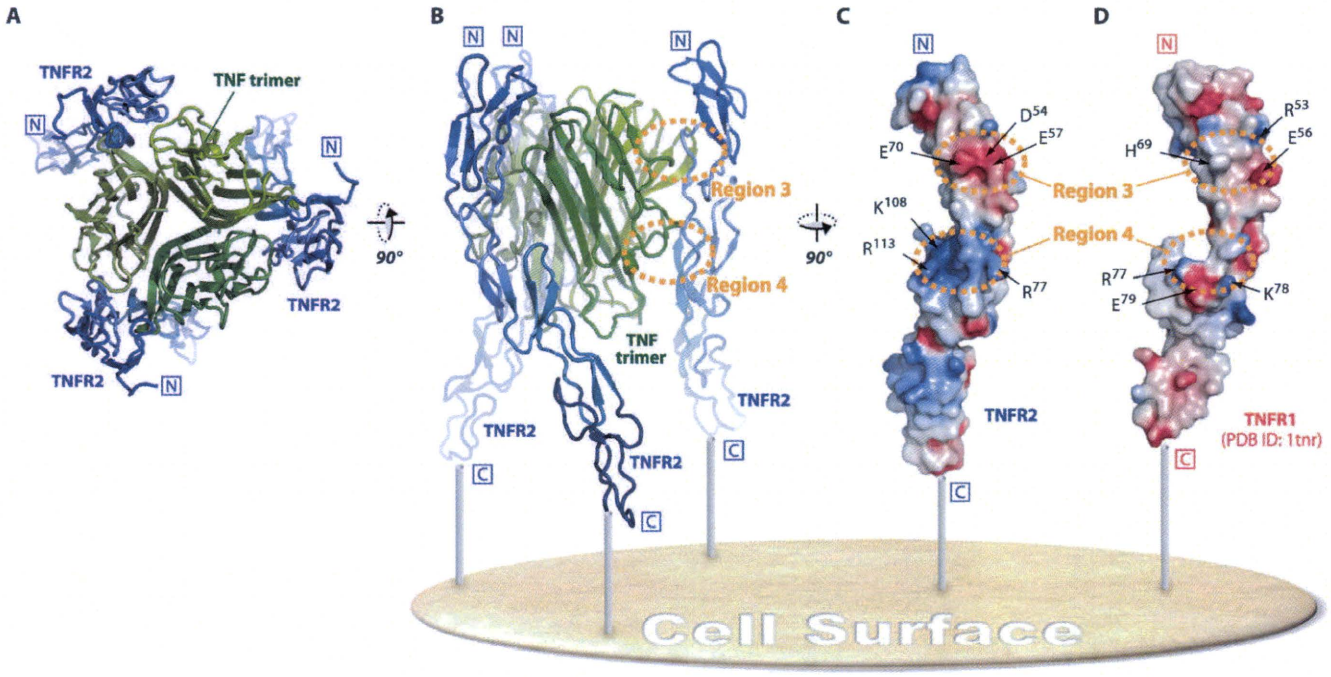

Fig. 3. Electrostatic surface potentials on the binding interfaces of TNFR2 and TNFR1. (**A** and **B**) Top view (A) and side view (B) of TNF-TNFR2 complexes (PDB ID 3alq). The TNF trimer is in green and the TNFR2 monomer is in blue. The binding regions (regions 3 and 4) are highlighted by orange, dashed circles. (**C**) Electrostatic surface potential of TNFR2. (**D**) Electrostatic surface potential of TNFR1 (PDB ID 1tnr). Each electrostatic surface potential was calculated with the GRASP program (*69*). Electrostatic charges (red indicates a negative charge, blue indicates a positive charge) are shown between $\pm 8 k_B T$, where k_B is the Boltzmann constant and T is the absolute temperature.

(Fig. 5C). By contrast, the longer loop structure of TNFR1 (residues Arg^{77} to Gly^{81}) was predicted to bind to TNF across a wide surface area by van der Waals contacts (Fig. 5D). This interaction is also observed in the structure of the LT-α–TNFR1 complex (*23*). These observations suggest that the loop motif in TNFR1 could be a focal point for creating new drugs that specifically inhibit the interaction between TNF and TNFR1.

A TNF-TNFR2 complex on the cell surface

Previous studies have confirmed that some members of the TNFR superfamily form a self-complex through their CRD1 (PLAD) regions at the cell surface, which also suggests that stimulation by ligand of these assemblies is necessary for efficient signaling (*32*, *33*). In the crystal structure of the TNF-TNFR2 complex, however, the CRD1 regions were separated from each other by >30 Å, which is too far to enable an interaction to occur. This phenomenon is also observed in other TNF-TNFR complexes (*23*, *26*–*29*). These apparently contradictory observations suggest that the binding of the TNF ligand induces a dynamic behavior in the TNFR self-complex that may trigger signal initiation.

To understand the state of TNFR2 at the cell surface, we transfected human embryonic kidney (HEK) 293T cells with plasmids encoding hemagglutinin (HA)–tagged wild-type TNFR2 (HA-wtTNFR2), TNFR2 lacking its PLAD (HA-TNFR2ΔPLAD), or TNFR2 lacking its intracellular domain (HA-TNFR2ΔCD). To identify self-complexes formed through PLAD-mediated interactions, we used the thiol-cleavable, membrane-impermeant, chemical cross-linker 3,3′-dithiobis(sulfosuccinimidyl propionate) (DTSSP), as described in a previous report (*33*). We performed Western blotting analysis of purified membrane fractions with antibody against HA to detect cross-linked, HA-tagged TNFR2 molecules. We observed a band corresponding to monomeric TNFR2 with a molecular mass of 65 kD (Fig. 6A, lanes 1 to 4). We also detected self-complexes of TNFR2 in the absence of TNF with molecular sizes about two or three times greater (130 or 195 kD) (Fig. 6A, lane 1), consistent with previous reports (*33*). Furthermore, analysis with high–molecular mass markers and a low-density polyacrylamide gel enabled us to identify a band of TNFR2 with a molecular mass of >1000 kD in samples treated with TNF (Fig. 6A, lane 2). These complexes were reduced to monomeric proteins by cleaving the cross-linker with dithiothreitol (DTT) (Fig. 6A, lanes 3 and 4). A similar experiment with cells transfected with plasmid encoding HA-TNFR2ΔPLAD revealed that the formation of TNFR2 self-complexes in the presence and absence of TNF was inhibited by the deletion of PLAD (Fig. 6A, lanes 5 and 6). In addition, treatment with TNF did not induce a shift in the band corresponding to HA-TNFR2ΔPLAD (Fig. 6A, lane 6), suggesting that most of the TNF did not bind to TNFR2 without PLAD at the cell surface. A previous report showed that deletion of the PLAD from TNFR1 markedly decreases the amount of TNF that binds to cell surface TNFR1 (*33*). Thus, our result suggests that the binding of TNF to TNFR2 is also disrupted by the deletion of the PLAD from TNFR2. In experiments with cells transfected with plasmid encoding HA-TNFR2ΔCD, we showed that this mutant TNFR could still form self-complexes (Fig. 6A, lane 9); however, the band corresponding to HA-TNFR2ΔCD did not shift upon treatment with TNF (Fig. 6A, lane 10). These results suggest that self-complexes of TNFR2 are formed through its PLAD on the surface of cells and that the stimulation of TNF was important for the formation of high–molecular mass aggregates of TNFR2.

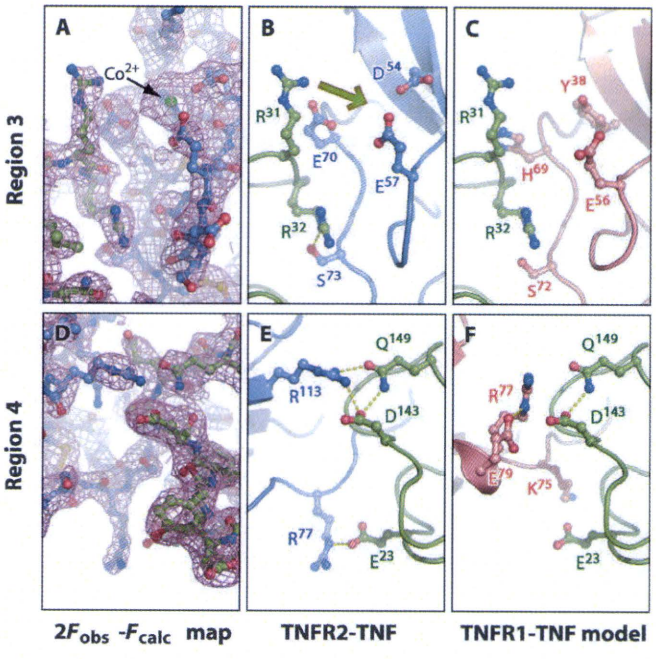

Fig. 4. Difference in the mode of binding of TNF to TNFR1 and TNFR2. Details of the ligand-receptor binding interfaces of TNF-TNFR are shown. (**A** and **D**) $2F_{obs} - F_{calc}$ map of the TNF-TNFR2 complex contoured at 1.0 σ. (**B** and **E**) The TNF-TNFR2 complex. The predicted interaction between R31 of TNF and the acidic surface of TNFR2 (consisting of D54, E57, and E70) is shown as a green arrow. (**C** and **F**) The TNF-TNFR1 model complex. To construct the TNF-TNFR1 model complex, we superimposed the LT-α portion of the LT-α–TNFR1 complex (PDB ID 1tnr) (*23*) onto the TNF portion of the TNF-TNFR2 structure. TNF is in green; TNFR1 is in red; TNFR2 is in blue; the $2F_{obs} - F_{calc}$ map is represented by the pink mesh. Close contacts that are suggestive of potential hydrogen bonds are represented by yellow dashed lines.

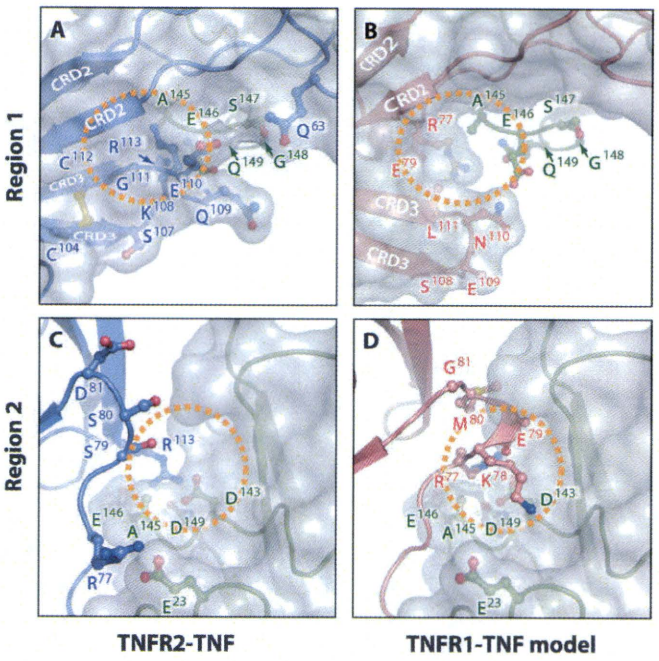

Fig. 5. TNF-TNFR complexes contain a molecular pocket. Difference in the basic structures of TNFR1 and TNFR2. (**A** and **C**) The TNF-TNFR2 complex. (**B** and **D**) The TNF-TNFR1 model complex, which was constructed as described in Fig. 4. TNF is in green; TNFR1 is in red; TNFR2 is in blue. The β strands of CRD2 and CRD3 are indicated by white text. The side chain of Glu^{109} is missing in the structure of TNFR1 (PDB ID 1tnr). We observed that a distinct molecular pocket was formed in (B) and (C), which is highlighted by an orange dashed circle.

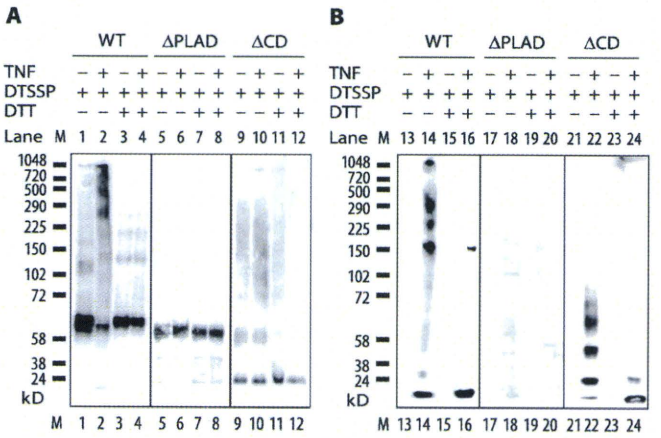

Fig. 6. Formation of TNF-TNFR2 aggregates on the cell surface. (**A** and **B**) TNF-TNFR2 complexes in the plasma membrane of transfected HEK 293T cells were detected by Western blotting analysis with antibodies against (A) the HA epitope and (B) TNF. This result was confirmed by three independent experiments for each group. Predicted molecular masses of related molecules are as follows: HA-wtTNFR2 monomer, 65 kD; HA-wtTNFR2 dimer, 130 kD; HA-wtTNFR2 trimer, 195 kD; TNF monomer, 17 kD; TNF trimer, 51 kD; HA-TNFR2ΔPLAD monomer, 60 kD; HA-TNFR2ΔCD monomer, 25 kD.

We also analyzed the same samples by Western blotting with an antibody against TNF (Fig. 6B). We observed high–molecular mass, TNF-specific bands of >150 kD in samples containing HA-wtTNFR2 and TNF (Fig. 6B, lane 14), but saw only monomeric TNF (17-kD band) under reducing conditions (Fig. 6B, lane 16). This result suggests that TNF molecules were contained in the aggregates of TNFR2 that we observed earlier (Fig. 6A, lane 2). In similar experiments with cells containing HA-TNFR2ΔPLAD, we did not observe TNF-specific bands in any group (Fig. 6B, lanes 17 to 20), indicating that TNF bound rarely to TNFR2ΔPLAD, as was predicted from our earlier results (Fig. 6A). These findings suggest that TNF bound to the PLAD-dependent self-complex of TNFR2 and that the PLAD was a key domain in forming a TNF-TNFR2 aggregate on the cell surface. We could not observe TNF within the self-complex of HA-TNFR2ΔCD (Fig. 6, A and B), indicating that the intracellular domain of TNFR2 also played an important role in forming the TNF-TNFR2 aggregate on the cell surface.

DISCUSSION

Here, we described the first crystal structure of the TNF-TNFR2 complex at a resolution of 3.0 Å. TNF formed a central homotrimer around which were bound three TNFR2 molecules. This overall arrangement was similar